Biochemical Genetics
https://doi.org/10.1007/s10528-024-11012-z

ORIGINAL ARTICLE

The Relationship Between Differential Expression of Non-coding RNAs (TP53TG1, LINC00342, MALAT1, DNM3OS, miR-126-3p, miR-200a-3p, miR-18a-5p) and Protein-Coding Genes (*PTEN, FOXO3*) and Risk of Idiopathic Pulmonary Fibrosis

Gulnaz F. Korytina[1,2] · Vitaly A. Markelov[1,2] · Irshat A. Gibadullin[2] · Shamil R. Zulkarneev[2] · Timur R. Nasibullin[1] · Rustem H. Zulkarneev[2] · Arthur M. Avzaletdinov[2] · Sergey N. Avdeev[3] · Naufal Sh. Zagidullin[2]

Received: 22 July 2024 / Accepted: 20 December 2024

Abstract

Idiopathic pulmonary fibrosis (IPF) is a rapidly progressive interstitial lung disease of unknown pathogenesis with no effective treatment currently available. Given the regulatory roles of lncRNAs (TP53TG1, LINC00342, H19, MALAT1, DNM3OS, MEG3), miRNAs (miR-218-5p, miR-126-3p, miR-200a-3p, miR-18a-5p, miR-29a-3p), and their target protein-coding genes (*PTEN, TGFB2, FOXO3, KEAP1*) in the TGF-β/SMAD3, Wnt/β-catenin, focal adhesion, and PI3K/AKT signaling pathways, we investigated the expression levels of selected genes in peripheral blood mononuclear cells (PBMCs) and lung tissue from patients with IPF. Lung tissue and blood samples were collected from 33 newly diagnosed, treatment-naive patients and 70 healthy controls. Gene expression levels were analyzed by RT-qPCR. TaqMan assays and TaqMan MicroRNA assay were employed to quantify the expression of target lncRNAs, mRNAs, and miRNAs. Our study identified significant differential expression in PBMCs from IPF patients compared to healthy controls, including lncRNAs MALAT1 (Fold Change = 3.809, $P = 0.0001$), TP53TG1 (Fold Change = 0.4261, $P = 0.0021$), and LINC00342 (Fold Change = 1.837, $P = 0.0448$); miRNAs miR-126-3p (Fold Change = 0.102, $P = 0.0028$), miR-200a-3p (Fold Change = 0.442, $P = 0.0055$), and miR-18a-5p (Fold Change = 0.154, $P = 0.0034$); and mRNAs FOXO3 (Fold Change = 4.604, $P = 0.0032$) and PTEN (Fold Change = 2.22, $P = 0.0011$). In lung tissue from IPF patients, significant expression changes were observed in TP53TG1 (Fold Change = 0.2091, $P = 0.0305$) and DNM3OS (Fold Change = 4.759, $P = 0.05$). Combined analysis of PBMCs expression levels for TP53TG1, MALAT1, miRNA miR-126-3p, and *PTEN* distinguished IPF patients from healthy controls with an AUC = 0.971, sensitivity = 0.80, and specificity = 0.955 ($P = 6 \times 10^{-8}$). These findings suggest a potential involvement of

Extended author information available on the last page of the article

Published online: 29 January 2025

the identified ncRNAs and mRNAs in IPF pathogenesis. However, additional functional validation studies are needed to elucidate the precise molecular mechanisms by which these lncRNAs, miRNAs, and their targets contribute to PF.

Keywords Idiopathic pulmonary fibrosis · lncRNA · miRNAs · mRNAs · TP53TG1 · MALAT1 · miR-126-3p · *PTEN*

Introduction

Pulmonary fibrosis (PF) is a pathological process characterized by the replacement of normal lung parenchyma with dense connective (fibrotic) tissue, driven by increased extracellular matrix synthesis and fibroblasts proliferation. This leads to lung tissue remodeling and ultimately functional failure (Noble et al. 2012; Giacomelli et al. 2021). Idiopathic PF (IPF), a rapidly progressive interstitial lung disease of unknown etiology, remains without effective treatment options (Richeldi et al. 2017). Over the past three years, the emergence of COVID-19 has significantly increased the prevalence of secondary PF alongside IPF, with PF being one of the most severe complications following COVID-19 (George et al. 2020).

The pathogenesis and progression of IPF are closely linked to persistent damage to pulmonary epithelium and endothelium caused by environmental factors such as cigarette smoke, toxins, chemicals, and viruses. This damage results in complex interaction among intracellular signaling cascades and dysfunctions within immune, epithelial, and mesenchymal cells following fibroblast activation (Noble et al. 2012; Phan et al. 2021). Damaged epithelial and endothelial cells actively express TGF-β, which activates TGF-β/Smad3, Wnt/β-catenin, and PDGF-signaling pathways, inducing epithelial-mesenchymal transition (EMT) and endothelial-mesenchymal transition (EndMT) (Giacomelli et al. 2021; Phan et al. 2021; Podolanczuk et al. 2013). These cells begin to produce pro-fibrogenic markers such as α-smooth muscle actin (α-SMA), fibroblast-specific protein 1 (FSP1), collagen 1, and fibronectin, and are capable of transdifferentiating into fibrogenic myofibroblasts (Pardo and Selman 2021). Macrophages are also implicated in PF development, as they regulate fibroblast transdifferentiation and proliferation through the secretion of mediators including platelet-derived growth factor (PDGF), connective tissue growth factor (CTGF), fibroblast growth factors (FGF), insulin-like growth factor 1 (IGF-1), cytokines, chemokines, and matrix metalloproteases (MMPs) (Giacomelli et al. 2021; Perez-Favila et al. 2024). Dysregulated signaling pathways such as TGF-β1/Smad3/α-SMA, Wnt/β-catenin, PI3K/AKT, HIPPO/YAP, and P53 play pivotal roles in fibrogenesis and lung tissue remodeling (Ye and Hu 2021; Pardo and Selman 2021; Perez-Favila et al. 2024).

PF has been linked to the active secretion of TGF-β, IL-8, and IL-1β by alveolar macrophages, which further promotes EMT (Giacomelli et al. 2021; Xu et al. 2023; Wynn and Vannella 2016). Activation of the PI3K/AKT- and mTOR-signaling pathway has been shown to increase the resistance of fibroblasts and myofibroblasts to apoptosis, thereby facilitating fibrosis (Romero et al. 2016; Allen et al. 2020; Wang

et al. 2021). Recent evidence has identified genes such as *MUC5B, TERT, TERC, RTEL1, PARN, SFTPC*, and *SFTPA2* as contributors to development (Michalski and Schwartz 2021; Tirelli et al. 2022). Genome-wide association studies (GWAS) have further uncovered more than 20 genetic loci associated with IPF, including *TERC, TERT, DSP*, 7q22.1, *MUC5B, ATP11A, IVD, AKAP13, KANSL1, FAM13A*, *DPP9, DEPTOR, KIF15,* and *MAD1L1* (Noth et al. 2013; Fingerlin et al. 2013; Allen et al. 2020).

The regulation of disease development also involves epigenetic mechanisms, including DNA and histone methylation and acetylation, as well as non-coding RNAs (ncRNA) such as microRNAs (miRNAs), long non-coding RNAs (lncRNAs), and circularRNAs (circRNAs) (Tirelli et al. 2022). These ncRNAs play crucial roles in regulating intracellular signaling pathways and are significant subjects of study for understanding various pathological phenotypes (Derrien et al. 2012; Kopp and Mendell 2018). Of particular scientific interest, lncRNAs, single-stranded RNAs longer than 200 bases, are actively investigated for their roles in fibrosis across multiple organs (Zhang et al. 2019, 2021; Sun et al. 2022). In the nucleus, lncRNAs contribute to nuclear compartmentalization, splicing regulation, and gene activity modulation through interactions with transcription factors, inhibition of their active sites, or by maintaining euchromatin and forming heterochromatin regions (Derrien et al. 2012; Long et al. 2017). In the cytoplasm, lncRNAs function as competing endogenous RNAs (ceRNAs) by binding to miRNAs, thereby preventing the suppression of messenger RNA (mRNAs). Additionally, they regulate the post-translational protein modifications, act as scaffolds for signaling pathway proteins, and participate in intercellular communication (Derrien et al. 2012; Ferrè et al. 2016). MiRNAs, on the other hand, are short ncRNAs (19–25 nucleotides) that regulate protein-coding gene expression by binding to target mRNAs, leading to translational inhibition or mRNA degradation (Usman Pp and Sekar 2024). Together, ncRNAs serve as key regulatory molecules controlling the genome at transcriptional and post-transcriptional levels. Profiling the expression of lncRNAs and miRNAs offers new insights into the molecular pathogenesis of complex diseases, including IPF (Boateng and Krauss-Etschmann 2020).

Studies suggest that ncRNAs have significant potential as clinically relevant biomarkers (Boateng and Krauss-Etschmann 2020; Poulet et al. 2020). Research has identified miRNAs, lncRNAs, and circRNAs as key regulators of intracellular signaling pathways implicated in IPF development (Zhang et al. 2021; Usman et al. 2021; Yan et al. 2017; Ali et al. 2022; Miao et al. 2018). Altered ncRNA expression plays a crucial role in initiating EMT and fibrosis (Qian et al. 2019; Xu et al. 2021). Transcriptomic studies have demonstrated differential expression of mRNAs and ncRNAs in PF models, identifying potential lncRNA–miRNA–mRNA networks involved in fibrotic process (Liu et al. 2020).

Thus, a wide array of molecules, cellular processes, signaling pathways, and regulatory elements have been implicated in IPF pathogenesis (Ali et al. 2022; Ye and Hu 2021). Unraveling the molecular mechanisms driving IPF, identifying biomarkers, and understanding its progression remain central to research efforts (Spagnolo and Lee 2023). Despite significant progress, the precise mechanisms underlying IPF pathogenesis are yet to be fully elucidated.

In the present study, we began by selecting lncRNAs previously linked to various fibrotic diseases or cancers, given the observed co-occurrence of lung cancer in IPF patients. This overlap may stem from the activation of shared signaling pathways (Podolanczuk et al. 2013; Lin et al. 2022; Yue et al. 2024). Six LncRNAs were chosen for investigation: TP53TG1, LINC00342, H19, MALAT1, DNM3OS, and MEG3.

TP53TG1 (TP53 target 1), located on chromosome 7q21 (https://www.ncbi.nlm.nih.gov/gene/11257/), is induced by the tumor suppressor protein p53, which mediates cellular responses to damage and participates in the TP53-signaling pathway (Lu et al. 2021). Studies have implicated TP53TG1 in pathways such as PRDX/WNT/β-catenin (Chen et al. 2021a), ERK1/ERK2 in hepatocellular carcinoma (Lu et al. 2021), and PI3K/AKT in breast cancer (Shao et al. 2020). In addition, its role in the pathogenesis of non-small cell lung cancer (NSCLC) has been noted (Yuan et al. 2017). TP53TG1 has also been identified as an antifibrotic factor (Sun et al. 2022).

LINC00342 (long intergenic non-protein-coding RNA 342), located on chromosome 2q11.1 (https://www.ncbi.nlm.nih.gov/gene/150759/), shows elevated expression in NSCLC tissues (Wang et al. 2016). It binds to miR-203a-3p (Chen et al. 2019c) and inhibits the tumor-suppressive activity of p53 and PTEN (Tang et al. 2019). Activation of the miR-15b/TPBG pathway by LINC00342 has been linked to lung adenocarcinoma progression, metastasis, and (Su et al. 2022).

H19 (H19 imprinted maternally expressed transcript), found on chromosome 11p15.5 (https://www.ncbi.nlm.nih.gov/gene/283120/), is expressed solely from the maternal chromosome (Ghafouri-Fard et al. 2020). H19 plays a pro-oncogenic role in cancers such as esophageal, gastric, rectal, and pancreatic cancers, including lung cancer (Yang et al. 2021a). It has also been implicated in pulmonary, cardiac, hepatic, and renal fibrosis (Jiang and Ning 2020).

MALAT1 (metastasis associated lung adenocarcinoma transcript 1), located on chromosome 11q13.1 (https://www.ncbi.nlm.nih.gov/gene/378938/), is expressed in various tissues and regulates the development of the nervous and muscular systems as well as vascular growth (Zhang et al. 2017a, b). Its oncogenic effects are mediated through signaling pathways such as MAPK/ERK, PI3K/AKT, beta-catenin/Wnt, Hippo, vascular endothelial growth factor (VEGF), and yes-associated protein (YAP) (Goyal et al. 2021). MALAT1 promotes cytokine production, fibroblast proliferation, migration, and EMT, exerting a pronounced pro-fibrotic effect in the lungs, liver, heart, and kidneys (Li et al. 2018a).

DNM3OS (DNM3 opposite strand/antisense RNA), located on chromosome 1q24.3 (https://www.ncbi.nlm.nih.gov/gene/100628315/), encodes an ncRNA that includes sequences for miR-199a-5p, miR-199a-3p, and miR-214–3 (Savary et al. 2019). DNM3OS acts as a fibroblast-specific downstream effector of TGF-β, driving lung fibrosis (Chen et al. 2015). It also promotes fibrosis in the lungs, heart, and liver (Chen et al. 2015; Kong et al. 2021) and is involved in the Hippo signaling pathway, which regulates cell proliferation and apoptosis (Yin et al. 2021).

MEG3 (maternally expressed gene 3), located on chromosome 14q32.2 (https://www.ncbi.nlm.nih.gov/gene/55384/), primarily exhibits tumor-suppressive effects. Reduced MEG3 expression has been observed in prostate (Wu et al. 2019), breast,

liver, colon, and lung cancers (Al-Rugeebah et al. 2019). Its role in fibrosis has also been explored, including its regulation of the mitochondrial apoptosis pathway through p53 activation and Bcl-xl inhibition (Gokey et al. 2018; Al-Rugeebah et al. 2019). MEG3 expression decreases during liver fibrosis (Yu et al. 2018), while its overexpression has been shown to inhibit TGF-β1-induced EMT, cell proliferation, and collagen synthesis (Xue et al. 2019; Zhan et al. 2021). MEG3 also contributes to lung tissue remodeling in IPF (Gokey et al. 2018).

The miRNAs interacting with the lncRNAs TP53TG1, LINC00342, H19, MALAT1, DNM3OS, and MEG3 selected for this study, were identified using online databases, including DIANA Tools/DIANA-LncBase v3 (diana.e-ce.uth.gr/LncBase v3.0), StarBase or ENCORI: Decoding the Encyclopedia of RNA Interactomes (https://rnasysu.com/encori/) (Li et al. 2014), and Lncrna2target V3.0 (http://bio-computing.hrbmu.edu.cn/lncrna2target/index.jsp) (Cheng et al. 2019). Among these, five miRNAs – miR-218-5p, miR-126-3p, miR-200a-3p, miR-18a-5p and miR-29a-3p – were chosen for the detailed analysis.

MiR-218-5p was identified as a regulator of the protein-coding genes *PTEN, TGFB2, FOXO3,* as well as lncRNA MEG3. This miRNA influences key biological pathways, including EMT, inflammation, and apoptosis (Chen et al. 2021c; Shan et al. 2022; Song et al. 2020). MiR-126-3p targets multiple genes implicated to carcinogenesis and inflammation, mediating the PI3K/AKT/mTOR pathway (Ebrahimi et al. 2014), apoptosis (Chen et al. 2021b), EMT, and fibrosis (Jordan et al. 2021). MiR-200a-3p is extensively studied for its role in regulating EMT, cell proliferation, and apoptosis. It is associated with pathways such as NF-κB- pathway (Cavallari et al. 2021), TGF-β-TGFR-SMAD (Hoffmann et al. 2016), Keap1/Nrf2 (Yu et al. 2019), and PI3K/AKT/mTOR (Shen et al. 2020). Notably, lncNAs MALAT1 and H19 modulate miR-200a-3p post-transcriptionally (Cavallari et al. 2021). MiR-18a-5p is a critical regulator of pathways such as TGF-β-SMAD2/3, PI3K/AKT, and WNT/β-catenin, which are involved in apoptosis, autophagy, EMT, and cellular stress responses (Kolenda et al. 2020; Zhong et al. 2023; Xiao and He 2020). The miR-29 family, particularly miR-29a-3p, regulates apoptosis and cell proliferation by targeting the TGF-β signaling pathway (Smyth et al. 2022), EMT (Wang et al. 2019a), and PI3K/AKT/mTOR pathway (Yang et al. 2021b). Importantly, miR-29 is pivotal in fibrosis development by modulating multiple signaling pathways and directly inhibiting genes encoding extracellular matrix proteins (Smyth et al. 2022).

For miRNA target gene prediction and pathway enrichment analysis, databases such as Target Scan Human Release 8.0 (http://www.targetscan.org) (McGeary et al. 2019), miRPath v4.0 (http://62.217.122.229:3838/app/miRPathv4), and miRwalk (http://mirwalk.umm.uni-heidelberg.de/) were employed. LncRNA–mRNA interaction analyses utilized StarBase/ENCORI (https://rnasysu.com/encori/) (Li et al. 2014) and Lncrna2target V3.0 (http://bio-computing.hrbmu.edu.cn/lncrna2target/index.jsp) (Cheng et al. 2019) also were used.

Four genes – *PTEN, TGFB2, FOXO3,* and *KEAP1* – were selected for further expression analysis. *PTEN* (Phosphatase and Tensin Homolog), located on chromosome 10q23, encodes a protein that antagonizes the PI3K/AKT/mTOR pathway, influencing glucose, lipid, and mitochondrial metabolism (Cai et al. 2022; Chen et al. 2018). *TGFB2* (Transforming Growth Factor Beta 2), located on chromosome

1q41 (https://www.ncbi.nlm.nih.gov/gene/7042), encodes a cytokine from the TGF-β family involved in cell proliferation, differentiation, migration, regeneration, apoptosis, intercellular matrix remodeling, and EMT (Ishtiaq Ahmed et al. 2014). The TGF-β family activates the canonical TGF-β/SMAD2/SMAD3/SMAD4 signaling pathway (Schepers et al. 2018). *FOXO3* (Forkhead Box O3), located on chromosome 6q21 (https://www.ncbi.nlm.nih.gov/gene/2309), encodes a transcription factor regulated by the PI3K/AKT-signaling pathway, which controls autophagy and apoptosis (Stefanetti et al. 2018). *KEAP1* (Kelch-like ECH-Associated Protein 1), located on chromosome 19p13.2 (https://www.ncbi.nlm.nih.gov/gene/9817), encodes an inhibitor of the transcription factor Nrf2 (NFE2 like bZIP transcription factor 2). The KEAP1-NRF2 complex is crucial for regulating oxidative homeostasis, senescence, and cell survival (Bellezza et al. 2018).

In this study, we focused on functionally interrelated lncRNAs, miRNAs, and target mRNAs implicated in the regulation of key pathways – TGF-β/Smad3, Wnt/β-catenin, focal adhesion, and PI3K/AKT/mTOR – recognized for their pivotal role in fibrogenesis. Those molecules were selected based on their predicted or experimentally validated interactions, encompassing lncRNAs-miRNA and miRNA-mRNA networks.

Given the invasive nature of lung biopsy and its associated high risks of morbidity and mortality, especially in the context of severe IPF (Gao et al. 2017), investigating gene expression in PBMCs offers a valuable non-invasive alternative for biomarker discovery (Gao et al. 2017). PBMCs, as immunocompetent cells, are critical players in the pathogenesis of respiratory diseases (Scott et al. 2019; Wynn and Vannella 2016; Schott et al. 2020). Among these, monocytes, which differentiate into alveolar macrophages upon injury, play a central role in fibrosis development (Podolanczuk et al. 2013; McCubbrey and Janssen 2024). The M2 phenotype of alveolar macrophages secretes inflammatory mediators and TGF-β, promoting pro-fibrotic processes and facilitating inflammatory cell recruitment, thereby driving fibrosis progression (Xu et al. 2023; Wynn and Vannella 2016). Elevated monocyte counts have been linked to higher mortality risk in IPF patients (Scott et al. 2019), while monocyte-derived alveolar exhibit increased expression of pro-inflammatory and pro-fibrotic genes (Misharin et al. 2017).

Recent single-cell RNA sequencing on PBMCs has identified an increased proportion of monocytes and regulatory T-cells in IPF patients, highlighting a lung–blood immune recruitment axis (Unterman et al. 2024). Numerous studies underline the potential of peripheral blood biomarkers, including gene expression profiles in PBMCs, for early-stage IPF diagnosis and effective disease monitoring (Yang et al. 2012a; Herazo-Maya et al. 2013). PBMCs, as key immune cells involved in cell–cell interactions, reflect lung-specific changes in IPF (Herazo-Maya et al. 2013; Fraser et al. 2021; Ishii et al. 2024).

Considering the functional significance of the selected ncRNAs and mRNAs in the TGF-β1/Smad, PI3K/AKT, focal adhesion, and Wnt/β-catenin signaling pathways, we aimed to evaluate the expression level of lncRNAs (TP53TG1, LINC00342, H19, MALAT1, DNM3OS, MEG3), miRNAs (miR-218-5p, miR-126-3p, miR-200a-3p, miR-18a-5p, miR-29a-3p), and target protein-coding genes (*PTEN, TGFB2, FOXO3, KEAP1*) in PBMCs and lung tissue of IPF patients.

Notably, this represents the first study to examine lncRNA, miRNA, and mRNA expression in IPF patients from the Volga-Ural region of Eurasia.

Materials and Methods

This study was conducted at Bashkir State Medical University (Ufa, Volga-Ural region of Eurasia, Russian Federation) between September 2022 and April 2024, adhering to the principles of Good Clinical Practice and the Declaration of Helsinki. Ethical approval was granted by the Ethics Committee of the Bashkir State Medical University (21.09.2022, No. 3), and written informed consent was obtained from all participants.

Study Population

Patients with Idiopathic Pulmonary Fibrosis

IPF was diagnosed in accordance with the clinical guidelines established by the American Thoracic Society, European Respiratory Society, Japanese Respiratory Society, and the Latin American Thoracic Association (ATS/ERS/JRS/ALAT) (Raghu et al. 2022). Diagnosis relied on patterns of interstitial lung disease identified through high-resolution computed tomography (HRCT) and, when necessary, lung tissue biopsy. Surgical biopsy was recommended in cases presenting subpleural fibrosis in the lower lobes and reticular shadows on HRCT. According to ATS/ERS guidelines, surgical verification is advised for cases with "probable" fibrosis, while transbronchial lung biopsy is generally not recommended, favoring video-assisted thoracoscopy or open biopsy instead.

Following comprehensive evaluations, including HRCT and lung scintigraphy, patients underwent minimally invasive video-assisted thoracoscopic lung resection to account for disease severity and procedure risks. Linear marginal resections yielded 5 mm^3 tissue samples for histological, genetic, and molecular analyses. IPF was diagnosed for the first time in all included patients, who had not received prior specific treatment. Lung tissue and blood samples were collected from 33 patients diagnosed with IPF at the Department of Thoracic Surgery, University Clinic of Bashkir State Medical University.

Control Group

Samples from the control group were obtained from 70 individuals undergoing lung surgery due to chest trauma at the same institution. Group characteristics are detailed in Table 1.

Table 1 Characteristics of the studied groups

Parameters	Patients ($N=33$)	Control ($N=70$)	P
Age (Mean ± SD)	55.19 ± 10.22	48.46 ± 14.14	0.0547[a]
Female (*n*, %)	24 (72.73)	46 (65.71)	0.627[c]
Male (*n*, %)	9 (27.27)	24 (34.29)	
Non-smokers (*n*, %)	24 (72.73)	46 (65.71)	0.627[c]
Smokers (*n*, %)	9 (27.27)	24 (34.29)	
Pack/years for smokers (Mean ± SD)	20.5 ± 15.1	23.06 ± 16.48	0.7446[a]
BMI (Mean ± SD)	26.74 ± 6.044	25.77 ± 4.311	0.5177[a]
FEV1/FVC (%)	98.75	105.6	0.6588[b]
(Median (25–75% IQR))	(88.28–109)	(83.64–113.2)	
VC (%)	75.39	83.21	0.0001[b]
(Median (25–75% IQR))	(54.43–88.35)	(47.99—92.58)	
FEV1 (%)	75.85	82.1	0.0001[b]
(Median (25–75% IQR))	(48.04–84.3)	(52.13–90.02)	
Comorbidities (*n*, %)		–	–
Type 2 diabetes mellitus	3 (9.09)		
Cardiovascular disease	7 (21.21)		
Emphysema	5 (15.15)		

BMI: Body mass index, FEV1: forced expiratory volume in 1 s, VC: vital capacity, FVC: forced vital capacity, Pack/years: number of cigarettes per day X number of years smoked / 20, Mean ± SD: Mean and Std. Deviation, Median (25–75% IQR): median and interquartile range, P: P-value for [a]Student t-test, [b]Mann-Whitney U-test, [c]Pearson's Chi-square test

Sample Collection

Lung tissue and blood samples were collected in the Department of Thoracic Surgery. Tissue samples were immediately preserved in RNA*later* solution (Thermo Fisher Scientific Inc.) and stored at − 70 °C until analysis. Peripheral blood samples (4 mL) were collected in EDTA tubes, processed within an hour, and PBMCs were isolated using Ficoll-Paque density centrifugation. PBMCs isolation involved diluting 4 mL of blood with an equal volume of phosphate-buffered saline (PBS), overlaying the mixture onto 3 mL of Ficoll-Paque (GE, Cytiva), and centrifuging at $420 \times g$ for 30 min at room temperature. The PBMCs layer was extracted, washed twice with PBS, and suspended in TRIzol Reagent (Thermo Fisher Scientific Inc.) for RNA extraction.

RNA Extraction and Quality Assessment

Lung tissue samples (~5 mm^3) were homogenized using a 3D–homogenizer (Precellys 24, Bertin Technologies) in TRIzol Reagent. RNA extraction from both tissue and PBMCs samples was performed per the manufacturer's protocol (Thermo Fisher

Scientific Inc.). RNA concentration and purity were assessed using a Nanodrop 2000 spectrophotometer (Thermo Fisher Scientific Inc.), with acceptable A260/A280 ratios between 1.8 and 2.0. RNA integrity was verified by analyzing rRNA bands (28S and 18S) via electrophoresis on 1% agarose gel stained with ethidium bromide. All RNA samples were treated with DNase I (Thermo Fisher Scientific Inc.) to eliminate genomic DNA contamination.

Reverse Transcription and qRT-PCR Reactions for lncRNAs and mRNAs

Reverse transcription for lncRNAs and mRNAs was performed using the First-Strand cDNA Synthesis Kit for RT-qPCR (Thermo Fisher Scientific Inc.), following the manufacturer's protocol. Total RNA (30 ng) was reverse transcribed into cDNA using a random primer. The reaction mixture (20 µL) included 30 ng of template RNA, 1 µL random primers, 4 µL of 5×reaction buffer (250 mM Tris–HCl, pH 8.3, 250 mM KCl, 20 mM $MgCl_2$, 50 mM DTT), 1 µL RiboLock RNase inhibitor (20 units/µL), 2 µL 10 mM dNTP mixture, 1 µL RevertAid M-MuLV reverse transcriptase (200 units/µL), and nuclease-free water. The mixture was incubated at 25 °C for 5 min, 42 °C for 60 min, and 70 °C for 5 min. The resulting cDNA was stored at –70 °C for subsequent analysis.

Quantitative real-time PCR (qRT-PCR) was conducted on a QuantStudio 5 qPCR System (Thermo Fisher Scientific Inc.) using qPCRmix-HS Master Mix (Evrogen, Russia, https://evrogen.ru) according to the manufacturer's recommendations. Each 25 µL reaction mixture contained 1 µL cDNA, 1 µL gene specific primers (10 µM), 1 µL fluorescent probes (10 µM), 5 µL qPCRmix-HS Master Mix, and nuclease-free water. Gene expression levels were assessed using TaqMan Assays (Thermo Fisher Scientific Inc.), which included primers and fluorescent probes for the following targets: TP53TG1 (gene ID 11257, Hs03462134_m1), LINC00342 (gene ID 150759, Hs00864338_m1), H19 (gene ID 283120, Hs00399294_g1), MALAT1 (gene ID 378938, Hs00273907_s1), DNM3OS (gene ID 100628315, Hs01369625_m1), MEG3 (gene ID 55384, Hs00292028_m1), TGFB2 (gene ID 7042, Hs00234244_m1), PTEN (gene ID 5728, Hs02621230_s1), FOXO3 (gene ID 2309, Hs00818121_m1), and KEAP1 (gene ID 9817, Hs00202227_m1). Beta-2-microglobulin (B2M, gene ID 567, Hs00187842_m1) served as internal control. Each reaction was performed in triplicate with cycling conditions as follows: 3 min at 95 °C (initial hot start), followed by 40 cycles of 15 s at 95 °C (denaturation) and 1 min at 60 °C (annealing/elongation). Positive and negative controls ensured RT-PCR specificity and quality.

Reverse Transcription and qRT-PCR Reactions for miRNA

For miRNA analysis, reverse transcription reactions were carried out using the TaqMan MicroRNA Reverse Transcription Kit (Thermo Fisher Scientific Inc.). Total RNA (30 ng) was reverse transcribed into cDNA using target-specific stem-loop primers, the TaqMan MicroRNA assay (Thermo Fisher Scientific Inc.) for hsa-miR-218-5p (Assay ID: 000521), hsa-miR-126-3p (Assay ID: 002228), hsa-miR-200a-3p

(Assay ID: 000502), hsa-miR-18a-5p (Assay ID: 002422), hsa-miR-29a-3p (Assay ID: 002112), and RNU6B (U6) (Assay ID**:** 001093). The 20 µL reaction mixture included 30 ng template RNA, 1 µL target-specific stem-loop primer (10 µM), 4 µL a 5×reaction buffer, 1 µL RiboLock RNase inhibitor (20 units/µL), 2 µL 10 mM dNTP mixture, 1 µL RevertAid M-MuLV reverse transcriptase (200 units/µL), and nuclease-free water. Reactions were incubated at 16 °C for 30 min, 42 °C for 30 min, and 85 °C for 5 min, then stored at –70 °C. qRT-PCR was conducted in triplicate on a QuantStudio 5 qPCR System using qPCRmix-HS Master Mix (Evrogen, Russia, https://evrogen.ru) under the following conditions: 95 °C for 10 min (hot start), followed by 40 cycles of 15 s at 95 °C (denaturation) and 1 min at 60 °C (annealing/elongation). Target-specific primers and fluorescent probes from the TaqMan MicroRNA Assay were used, with RNU6B (U6) as the endogenous control. Positive and negative controls were included for validation and quality assurance.

LncRNA–miRNA–mRNA Interaction Analysis

Interaction among lncRNAs, miRNAs, and mRNAs were analyzed using StarBase (ENCORI) (https://rnasysu.com/encori/, accessed on September 2023) (Li et al. 2014) and Lncrna2target V3.0 (http://bio-computing.hrbmu.edu.cn/lncrna2target/index.jsp, accessed on September 2023) (Cheng et al. 2019). To identify miRNAs binding to the lncRNAs studied (TP53TG1, LINC00342, H19, MALAT1, DNM3OS, MEG3) data from DIANA Tools/ DIANA-LncBase v3 (diana.e-ce.uth.gr/ LncBase v3.0) were used (Paraskevopoulou et al. 2016). Target gene prediction for miRNAs was performed using multiple databases, including miRTarBase v8.0 (accessed on September 2023) (Huang et al. 2020), TarBase v8.0 (https://dianalab.e-ce.uth.gr/tarbasev9, accessed on September 2023), Target Scan Human database Release 8.0 (http://www.targetscan.org, accessed on September 2023) (McGeary et al. 2019) miRPath v4.0 from DIANA Tools (http://62.217.122.229:3838/app/miRPathv4, accessed on September 2023), and miRwalk (http://mirwalk.umm.uni-heidelberg.de/), which integrates results from 12 prediction tools. Pathway enrichment and network visualization were conducted using ShinyGO: a graphical gene-set enrichment tool (http://bioinformatics.sdstate.edu/go/, accessed on September 2023), STRING (https://string-db.org/, accessed on December 2023), Cytoscape software v.3.10.1 platform (https://cytoscape.org, accessed on December 2023), WikiPathways (https://www.wikipathways.org/, accessed on December 2023), NetworkAnalyst 3.0 (https://www.networkanalyst.ca/NetworkAnalyst/, accessed on September 2023), and KEGG (Kyoto Encyclopedia of Genes and Genomes) database (https://www.kegg.jp/).

Statistical Analysis

Statistical analyses were performed using MS Excel 2003, GraphPad Prism 9 (GraphPad Software, https://www.graphpad.com), and SPSS Statistics 22.0. Data normality was assessed using the Shapiro Wilk test. For quantitative variables, results were expressed as mean ± standard deviation (Mean ± SD) or median and

interquartile range (Median (25–75% IQR), and group comparisons were performed using nonparametric Mann–Whitney *U*-test (non-normal data) or Student's test (normal data). Categorical variables were analyzed using Pearson's Chi-square (χ^2) test.

Relative gene expression was calculated using the ΔΔCt method (Livak and Schmittgen 2001). Significant differences in expression level between patients and controls were evaluated using the Mann–Whitney *U*-test. Correlations among variables were analyzed using Spearman's rank correlation coefficient. Statistical significance was set at $P < 0.05$. Receiver operating characteristic (ROC) curve analysis was used to evaluate the diagnostic potential of lncRNAs, mRNAS, and miRNAs expression levels in IPF. Regression models were constructed to identify significant predictors, with ROC analysis employed to assess model performance.

Results

Demographic Characteristics of the Study Groups

The clinical and demographic characteristics of the study groups are presented in Table 1. The IPF patient group and the control were comparable in basic characteristics, including age, gender, smoking status, body mass index (BMI), and smoking intensity (pack/years for smokers). However, significant differences were observed in lung function parameters between the groups, specifically in Vital Capacity (VC) ($P = 0.001$) and Forced Expiratory Volume in 1 s (FEV1) ($P = 0.0001$) (Table 1).

As reported in the literature, respiratory and non-respiratory comorbidities frequently affect IPF patients, influencing disease severity and patient survival (Podolanczuk et al. 2013). In our cohort, the following comorbidities were observed: emphysema (15.15%), cardiovascular disease (21.21%), and type 2 diabetes (9.09%) (Table 1).

In Silico lncRNA–miRNA–mRNA Interaction Analysis and Pathway Enrichment Analysis

We conducted in silico analyses to identify interaction network among lnRNAs, miRNAs, and mRNAs. Table 2 summarizes the functional characteristics of the selected lncRNAs, mRNAs, and their interaction with miRNAs. Figures 1 and 2 illustrate the interactions of the studied miRNAs with lncRNAs and mRNAs. This study focused on miRNAs interacting with selected lncRNAs and their respective target mRNAs.

For example, miR-218-5p interacts with lncRNA MEG3 and protein-coding genes *PTEN, TGFB2*, and *FOXO3*. MiR-200a-3p target a wide range of genes, including *PTEN, TGFB2,* and *KEAP1*, while interacting with the lncRNAs MALAT1 and H19. Similarly, miR-18a-5p interacts with lncRNAs H19 and TP53TG1 and targets mRNAs *PTEN* and *FOXO3* (Figs. 1 and 2). Additionally, miR-29a-3p regulates various biological processes and target multiple genes, including *PTEN, TGFB2, FOXO3, KEAP1,* and lncRNAs H19 and DNM3OS. Notably, miR-29a-3p interacts

Table 2 LncRNA–miRNA–mRNA interaction analysis

RNA / gene	Molecular targets / interacting miRNAs	Function
TP53TG1	**miR-18a-5p**	Pro-apoptotic effect
	ACTA2, Fn1	Anti-fibrotic effect
LINC00342	miR-15b/TPBG, miR-15b/BCL2, miR-203a-3p/SIX1	Modulation of epithelial-mesenchymal transition
	miR-203a-3p	Modulation of lung inflammation
H19	miR-29b, **miR-29a-3p,** miR-196a, miR-140, miR-21/PTEN/AKT, **miR-18a-5p**	Pro-fibrotic effect, Anti-apoptotic effect
	miR-122-5p, **miR-29a-3p,** miR-140-5p/TLR4, miR-140-5p /TGFBR2	Modulation of lung inflammation
	miR-675-3p/IGF1R, **miR-200a**, miR-19b-3p/FTH1, miR-130a-3p/WNK3, miR-193a-3p	Anti-fibrotic effect
	miR-138, miR-29b-3p/STAT3, **miR-200a-3p**/ZEB1, miR-203a-3p/SIX1	Modulation of epithelial-mesenchymal transition
	miR-200b-3p, miR-101-3p/MCL1, miR-206 (Akt/mTOR pathway) miR-202-3p/RRM2, miR-202-3p/CCND1, miR-374b-5p/SRSF7, miR-129-5p/YWHAB, miR-613/COMMD8, miR-613/GJA1, miR-613/CDK4, miR-19b-3p/PPP2R5E, miR-19b-3p/BCL2L11, miR-17-5p/FOXA1, miR-1297/ TRIB2, miR-375/YAP;	Anti-apoptotic effect
	miR-194-5p/FOXP2	Pro-apoptotic effect
	miR-503-5p	Pro-fibrotic effect

Table 2 (continued)

RNA / gene	Molecular targets / interacting miRNAs	Function
MALAT1	miR-200b-3p, miR-101-3p/MCL1, miR-206 (Akt/mTOR pathway) miR-202-3p/RRM2, miR-202-3p/CCND1, miR-374b-5p/SRSF7, miR-129-5p/YWHAB, miR-613/COMMD8, miR-613/GJA1, miR-613/CDK4, miR-19b-3p/PPP2R5E miR-19b-3p/BCL2L11, miR-17-5p/FOXA1, miR-1297/ TRIB2, miR-375/YAP	Anti-apoptotic effect
	miR-194-5p/FOXP2	Pro-apoptotic effect
	miR-503-5p	Pro-fibrotic effect
	CCT4, CTHRC1, HMMR, DOT1, ABCA1, ADAMTS12, ADGRL2, BMPER, CA2, CDCP1, COL6A1, CPM, CSF1, CXCL5, DRD1, GPC6, HNF4G, LAYN, LPAR1, LY6K, MCAM, MIA2, NNMT, PRKCE, RASSF6, ROBO1, STC1, EZH2; miR-101/SOX9 (Wnt pathway), miR-206 (Akt/mTOR pathway), miR-202-3p/RRM2, miR-374b-5p/ SRSF7, miRNA-374b-5p/FOXP1, miR-129-5p/MCRS1, miR-129-5p/CDH1, miR-129-5p/VIM, miR-194-5p/FOXK1, miR-613, miR-590/YAP1, miR-150/eIF4E/Akt, miR-200 family: **miR-200a-3p,** miR-200b-3p, miR-200c-3p	Modulation of epithelial-mesenchymal transition
	miR-129-5p/ HMGB1, miR-22-3p/NLRP3, miR-375, miR-590	Modulation of lung inflammation
DNM3OS	miR-199a-5p/3p, miR-214-3p, miR-140-5p/MMD, miR-125a-5p/SIRT2, miR-125a-5p/BCL2, miR-125a-5p/HDAC1, miR-140-5p/YES1, miR-125a-5p/STAT3	Anti-apoptotic effect
	miR-199a-5p/3p/SIRT1, miR-181a-5p/STAT3	Modulation of lung inflammation
	miR-204-5p/AP1S2, miR-204-5p/ATG3	Pro-fibrotic effect
	miR-29a-3p	Modulation of epithelial-mesenchymal transition

Table 2 (continued)

RNA / gene	Molecular targets / interacting miRNAs	Function
MEG3	miR-181a-5p/Bcl-2, miR-140-5p/MMD, miR-125a-5p, miR-140-5p/YES1, miR-125a-5p/STAT3	Anti-apoptotic effect
	MDM2, p53	Pro-apoptotic effect
	TP63, KRT14, STAT3, YAP1, TP73, SOX2, HES1 and HEY1, MDM2 and p53, JARID2 and EZH2, miR-181a-5p/PTEN, miR-181b-5p, miR-133a-3p (TGF-β/Smad3 pathway), miR-133a-3p/ IGF1R, miR-140-5p (Wnt pathway), miR-181d-5p/CDKN3, miR-770-5p/TGFBR1	Modulation of epithelial-mesenchymal transition
	miR-181a-5p/PTEN/pSTAT5/SOCS1, miR-181b-5p/JAK2/STAT3, miR-133a-3p/SIRT1, miR-140-5p/ TLR4**, miR-218-5p**	Modulation of lung inflammation
TGFB2	miR-454-3p, **miR-218-5p, miR-200a-3p**	Modulation of epithelial-mesenchymal transition
	miR-193a-3p, **miR-29a-3p**	Anti-apoptotic effect, Pro-fibrotic effect
PTEN	miR-19b-3p, miR-23a-3p, miR-217-5p, miR-221-3p, miR-222-3p, miR-486-5p, miR-425-5p, **miR-18a-5p**, miR-543, miR-20b-5p, **miR-29a-3p**	Anti-apoptotic effect
	miR-21, miR-216a, **miR-29a-3p**	Pro-fibrotic effect
	miR-181a-5p, **miR-218-5p, miR-200a-3p**	Modulation of epithelial-mesenchymal transition
FOXO3	miR-182, miR-217, miR-29b-3p, **miR-29a-3p, miR-18a-5p**	Anti-apoptotic effect
	miR-23a, **miR-126-3p**	Pro-apoptotic effect
	miR-218-5p, miR-126-3p	Modulation of epithelial-mesenchymal transition
KEAP1	miR-421, miR-432-3p; miR-125b-5p, miR-141-3p, **miR-200a-3p,**	Anti-apoptotic effect and Pro-apoptotic effect
	miR-29a-3p	Modulation of lung inflammation

lncRNA–miRNA–mRNA interaction analysis was performed using KEGG (Kyoto Encyclopedia of Genes and Genomes) integrated database (https://www.kegg.jp/), miRTarBase v8.0 (Huang et al. 2020) and TarBase v9.0 (https://dianalab.e-ce.uth.gr/tarbasev9), starBase v2.0 (Li et al. 2014), NetworkAnalyst 3.0 (https://www.networkanalyst.ca/NetworkAnalyst/), Lncrna2target V3.0 (http://bio-annotation.cn/lncrna2target/browse.jsp) (Cheng et al. 2019). miRNAs selected for study are highlighted in bold

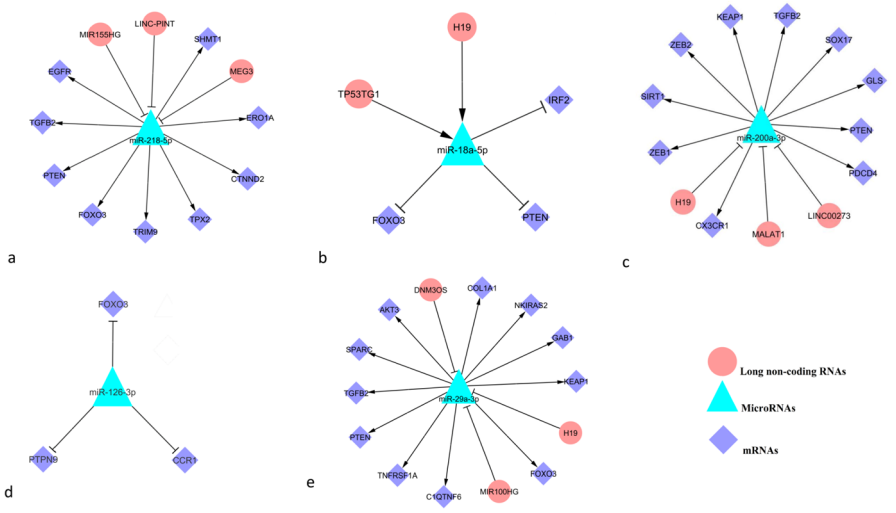

Fig. 1 Interaction network between miRNA and mRNA/lncRNAs. The Cytoscape 3.10.0 software platform was used to visualize complex networks. **a** miR-218-5p; **b** miR-18a-5p; **c** miR-200a-3p; **d** miR-126-3p; **e** miR-29a-3p

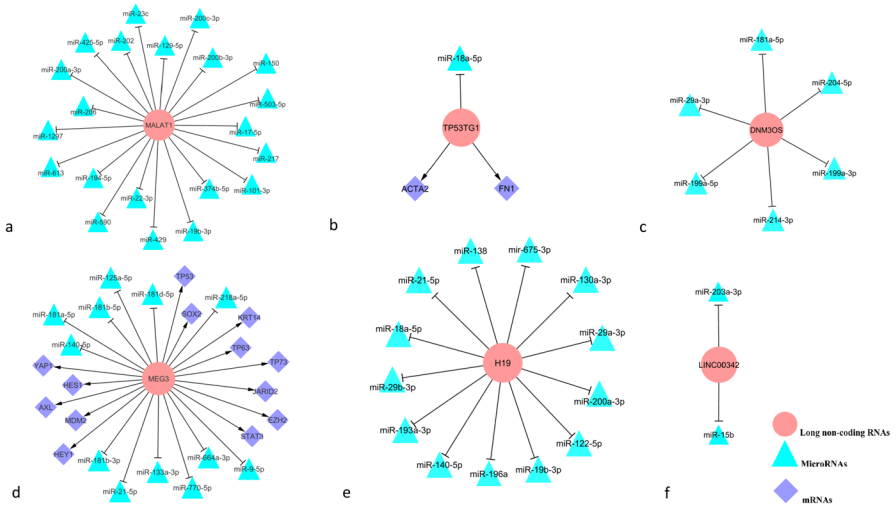

Fig. 2 Interaction network of studied lncRNAs. The Cytoscape 3.10.0 software platform was used to visualize complex networks. **a** MALAT1; **b** TP53TG1; **c** DNM3OS; **d** MEG3; **e** H19; **f** LINC00342

with *FOXO3* and other target genes in biological processes such as apoptosis and cellular senescence.

We employed miRPath v.4.0, ShinyGo (http://bioinformatics.sdstate.edu/go/), and STRING (https://string-db.org/) for the analysis of the target genes of the studied miRNAs. miRPath analysis, performed using the TarBase v8.0 database,

identified 116 signaling cascades (genes union method) and 111 signaling cascades (pathways union method), including key pathways such as PI3K/AKT signaling ($P = 5.2956e^{-15}$), focal adhesion ($P = 7.8367e^{-11}$), FoxO signaling ($P = 1.2488e^{-08}$), cellular senescence ($P = 3.9975e^{-07}$), Wnt signaling ($P = 0.00718011$), apoptosis ($P = 1.5598e^{-06}$), and mTOR signaling ($P = 0.00067967$), all implicated in IPF pathogenesis (Supplementary Fig. 1, Supplementary Table 1). Analysis using the microT-CDS algorithm identified 97 and 60 signaling cascades (genes union and signaling pathways union methods, respectively), with significant enrichment in pathways such as PI3K/AKT signaling, focal adhesion, FoxO signaling, apoptosis, Wnt signaling (Fig. 3, Supplementary Table 2).

Notably, miR-29a-3p and hsa-miR-218-5p contributed most significantly to pathway enrichment. Further analyses focused on 154 target genes within the PI3K/AKT-signaling pathway (merged data from TarBase v8.0 and microT-CDS). Hierarchical pathway correlation clustering (Supplementary Fig. 2b) revealed the most significant cluster centered on PI3K/AKT signaling ($P = 1.3e^{-278}$).

STRING analysis of protein–protein interactions (PPI) for miRNA target genes revealed a P-value $< 1.0e^{-16}$, indicating that the encoded proteins are biologically interconnected (Fig. 4, Supplementary Fig. 3). These genes are part of 174 KEGG pathways, including 152 genes involved in the PI3K/AKT-signaling cascade ($P = 6.35e^{-248}$, strength = 1.75). Analysis using WikiPathways identified 144 genes associated with PI3K/AKT signaling ($P = 1.07e^{-225}$, strength = 1.74) (Fig. 4). Key elements of these genes within the PI3K/AKT-signaling cascade are highlighted in Fig. 5.

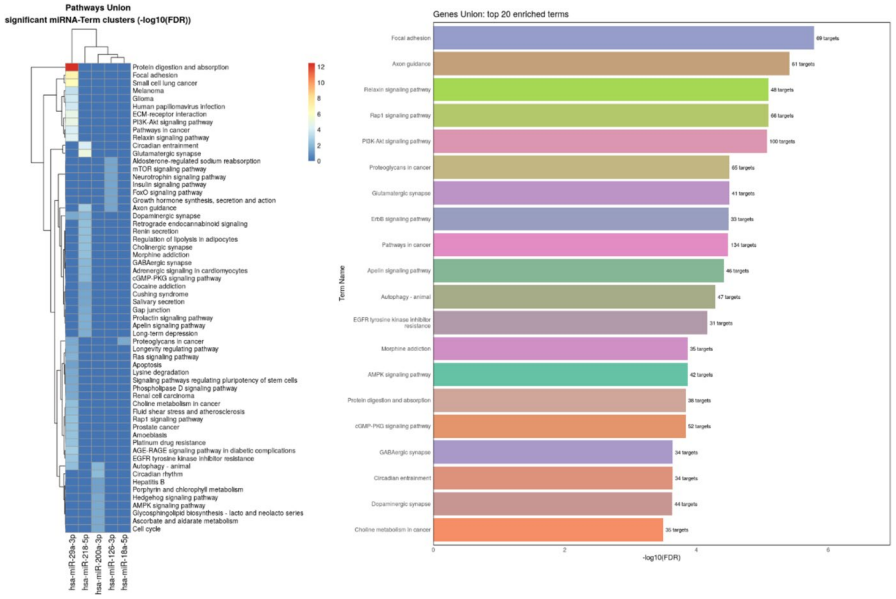

Fig. 3 Heat map of KEGG target pathways involving the studied miRNA target genes (based on the microT-CDS algorithm): **a** Pathways union method; **b** Genes union method (20 most significant signaling cascades included)

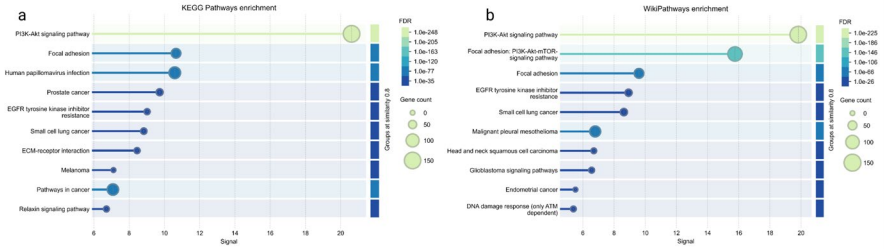

Fig. 4 Graphical representation the results of 154 target protein–protein interactions of target genes of investigated miRNAs (combined TarBase v8.0 and microT-CDS data) using STRING online resource: **a** Results of analysis using the KEGG pathway online resource; **b** Results of analysis using the WikiPathways online resource (https://www.wikipathways.org/)

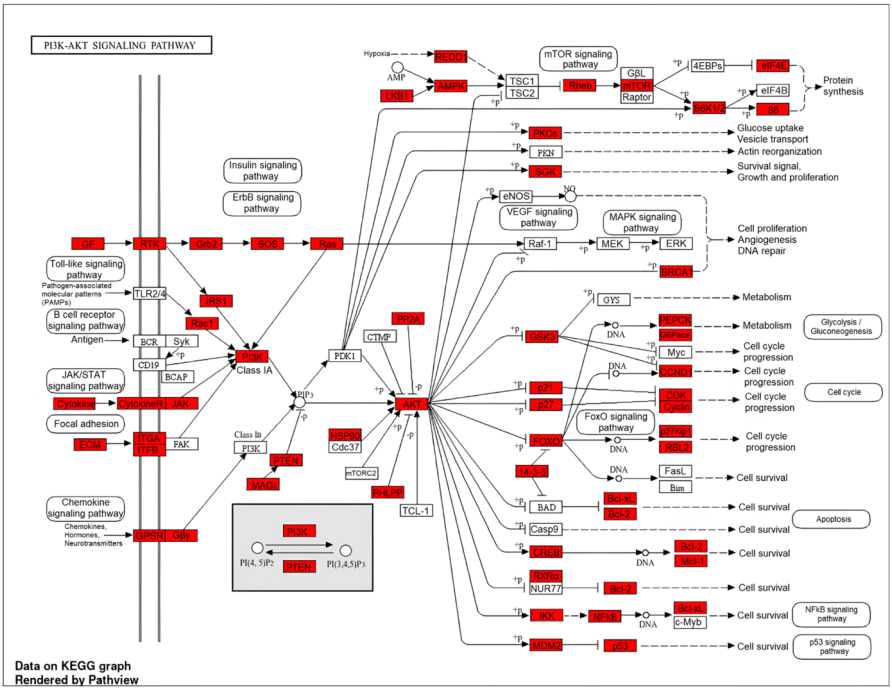

Fig. 5 Schematic illustration of the PI3K/AKT-signaling pathway based on KEGG data of analyzed miRNA targets. Genes identified as targets are highlighted in red

Using ENCORI/StarBase, ShinyGo, and STRING, we analyzed the target genes of the six lncRNAs under study. Enrichment analyses based on experimentally validated interactions from the ENCORI/StarBase platform were performed with specific parameters: ExpNum ≥ 1 for TP53TG1, LINC00342, H19, DNM3OS, and MEG3; and ExpNum ≥ 3 for MALAT1 to level the excess of target RNA. These lncRNAs have 1977 target RNAs (Supplementary Tables 4–9).

ShinyGo analysis (Supplementary Fig. 4a; Supplementary Table 10) identified the 20 most enriched signaling pathway targeted by the lncRNAs. Hierarchical clustering (Supplementary Fig. 4b) highlighted focal adhesion as a significant pathway (FDR = $3.6e^{-11}$). STRING analysis of PPI for lncRNA targets (P-value < $1.0e^{-16}$) confirmed biological interconnectivity (Supplementary Fig. 5). According to KEGG and WikiPathways data, lncRNA targets are involved in 72 and 74 pathways, respectively, with focal adhesion prominently represented (KEGG: FDR = $7.67e^{-07}$; strength = 0.45; WikiPathways: FDR = $5.56e^{-06}$; strength = 0.43) (Supplementary Fig. 6). The key elements of the focal adhesion signaling pathway, which are target products of the studied lncRNAs, are presented in Fig. 6.

Our analysis indicates that the miRNAs, lncRNAs, and target mRNAs included in the study function as regulators of PI3K/AKT/mTOR signaling, focal adhesion, FoxO-signaling pathway, apoptosis, Wnt signaling, TGF-β/SMAD3-signaling pathways. They are implicated in critical cellular processes, including EMT, apoptosis, antioxidant response to oxidative stress, inflammation, fibrogenesis, and cellular senescence.

Relative Expression of Studied lncRNAs, mRNAs, and miRNAs in Peripheral Blood Mononuclear Cells (PBMCs)

We analyzed the expression of lncRNAs (TP53TG1, LINC00342, H19, MALAT1, DNM3OS, MEG3), miRNA (miR-218-5p, miR-126-3p, miR-200a-3p, miR-18a-5p, miR-29a-3p), and protein-coding genes (*PTEN, TGFB2, FOXO3, KEAP1*) in PBMCs and lung tissue samples from both patients and control group.

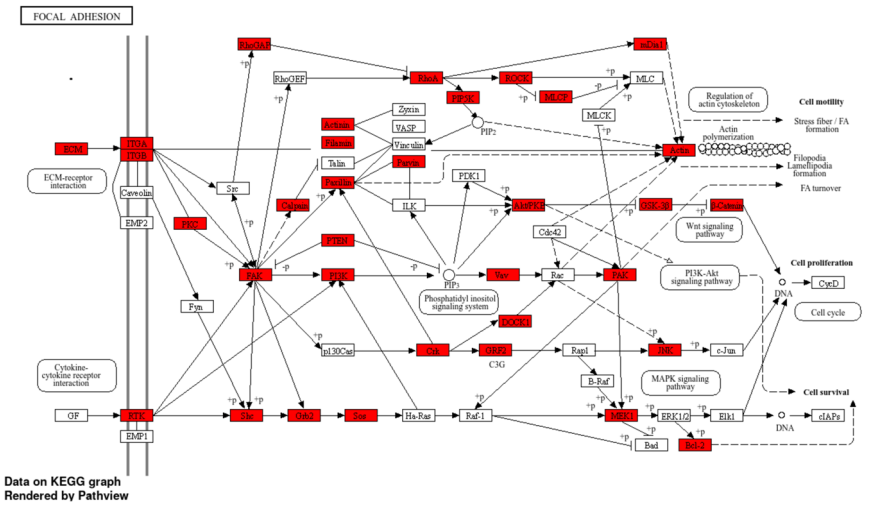

Fig. 6 Schematic representation of the Focal Adhesion signaling cascade based on KEGG data of analyzed lncRNA targets. Genes identified as targets are highlighted in red

Table 3 The expression profiles of selected lncRNAs, mRNAs, and miRNAs in peripheral blood mononuclear cells (PBMCs) and lung tissue samples of IPF patients

RNA	Peripheral blood mononuclear cells (PBMCs)			Lung tissue samples		
	Fold change ($2^{(-\Delta\Delta Ct)}$ case / $2^{(-\Delta\Delta Ct)}$ control)	Fold up- or down-regulation	*P*-value	Fold change ($2^{(-\Delta\Delta Ct)}$ case / $2^{(-\Delta\Delta Ct)}$ control)	Fold up- or down-regulation	*P*-value
TP53TG1	0.4261	-2.346	**0.0021**	0.2091	− 4.781	**0.0305**
LINC00342	1.837	1.837	**0.0448**	0.4733	− 2.112	0.8703
MALAT1	3.809	3.809	**0.0001**	2.979	2.979	0.6196
H19	5.45	5.45	0.06	3.186	3.186	0.9137
DNM3OS	3.41	3.41	0.091	4.759	4.759	**0.05**
MEG3	2.716	2.716	0.6121	5.001	5.001	0.5208
TGFB2	1.197	1.197	0.2302	0.892	− 1.12	0.667
PTEN	4.604	4.604	**0.0032**	1.59	1.59	0.1512
FOXO3	2.22	2.22	**0.0011**	0.128	− 7.77	0.5191
KEAP1	2.78	2.78	0.1281	1.469	1.469	0.94
miR-218-5p	3.954	3.954	0.1579	3.99	3.99	0.369
miR-126-3p	0.102	− 9.721	**0.0028**	2.969	2.969	0.096
miR-200a-3p	0.442	− 2.258	**0.0055**	0.28	− 3.55	0.841
miR-18a-5p	0.154	− 6.463	**0.0034**	0.806	− 1.23	0.665
miR-29a-3p	0.519	− 1.925	0.851	2.689	2.689	0.1733

P-value for Mann–Whitney test U-test; Fold Regulation for Fold Change < 1 calculated as (-1/ Fold Change). The statistically significant differences are highlighted in bold

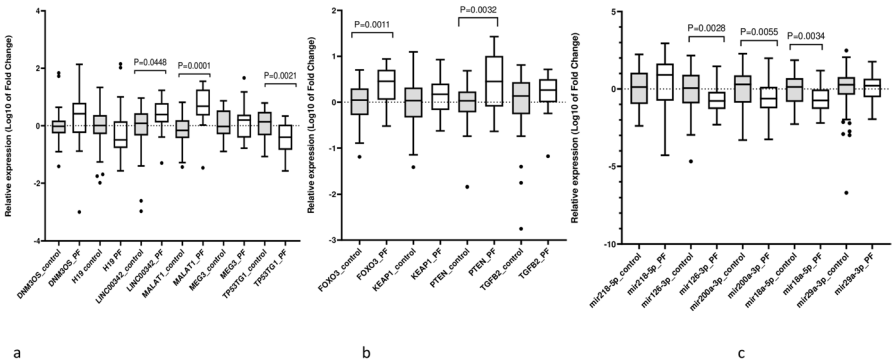

Fig. 7 Relative expression levels of lncRNAs (**A**), mRNAs (**B**), and miRNAs (**C**) in PBMCs of patient and control groups. Results presented as Log10 of Fold Change (Log10 $2^{-\Delta\Delta Ct}$) in Tukey box-and-whisker plots, P: P-value for Mann-Whitney *U*-test.

The lncRNAs differentially expressed in the PBMCs of IPF patients are presented in Table 3 and Fig. 7a. Notably, the relative expression of TP53TG1 was significantly downregulated in the PBMCs of IPF patients (Fold Change (FCh) = 0.4261, Fold Regulation (FR) = − 2.346, $P = 0.0021$). Conversely, LINC00342 (FCh = 1.837,

$P=0.0448$) and MALAT1 (FCh = 3.809, $P=0.0001$) were significantly upregulated in PBMCs of IPF patients. Among protein-coding genes *PTEN* (FCh = 4.604, $P=0.0032$) and *FOXO3* (FCh = 2.22, $P=0.0011$) showed a statistically significant increase in relative expression in IPF patients' PBMCs (Table 3 and Fig. 7b). Regarding miRNAs, three were differently expressed in the PBMCs of IPF patients (Table 3, Fig. 7c). The relative expression levels of miR-126-3p (FCh = 0.102, FR = − 9.721, $P=0.0028$), miR-200a-3p (FCh = 0.442, FR = − 2.258, $P=0.0055$), and miR-18a-5p (FCh = 0.154, FR = − 6.463, $P=0.0034$) were significantly downregulated in IPF patients.

Relative Expression of Studied lncRNAs, mRNAs and miRNAs in Lung Tissue

The expression profiles of lncRNAs, mRNAs, and miRNAs in lung tissue samples from IPF patients and controls are summarized in Table 3 and Fig. 7. In the lung tissue of IPF patients, TP53TG1 was significantly downregulated (FCh = 0.2091 FR = − 4.781, $P=0.0305$). Conversely, DNM3OS was notably upregulated (FCh = 4.759, $P=0.05$). However, no significant differences were observed in the expression levels of LINC00342, H19, MALAT1, miR-218-5p, miR-126-3p, miR-200a-3p, miR-18a-5p, miR-29a-3p, *PTEN, TGFB2, FOXO3,* and *KEAP1* between the lung tissue of IPF patients and controls. These findings may reflect the distinct expression patterns of ncRNA and mRNA across different cell types and tissues (Fig. 8).

Correlation Analysis

Considering the functional interactions among the selected lncRNAs, miRNAs, and mRNAs, we examined the correlations between their expression levels, as well as their relationships with clinical and demographic parameters in PBMCs and lung tissue samples. The findings are detailed in Supplementary Tables 11, 12, 13, 14 and

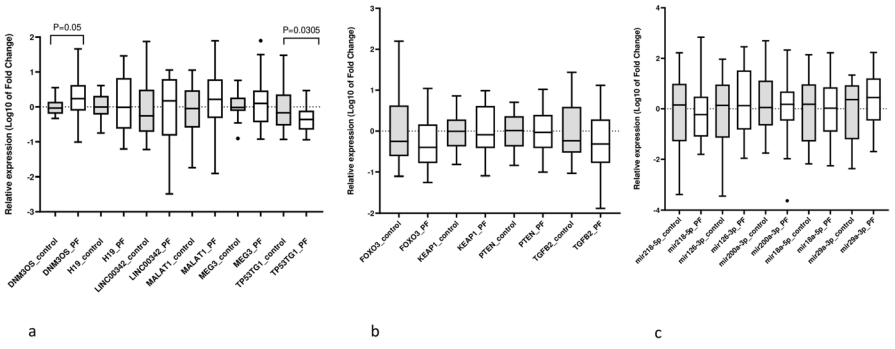

Fig. 8 Relative expression level of lncRNAs (**A**), mRNAs (**B**), and miRNAs (**C**) in lung tissue of patient and control groups. Results are presented as Log10 of Fold Change (Log10 $2^{-\Delta\Delta Ct}$) in Tukey box-and-whisker plots, *P*: *P*-value for the Mann-Whitney *U*-test.

visualized as heat maps in Supplementary Figs. 7 and 8. The most significant correlations between the relative expression level of all studied lncRNAs, miRNAs, and mRNAs in PBMCs and lung tissue are highlighted in Fig. 9. Correlations between clinical/demographic parameters and the relative expression levels of these molecules are illustrated in Fig. 10.

Several notable correlations were observed. In PBMCs, DNM3OS expression showed a positive correlation with H19 (r = 0.311, $P = 0.047$). TP53TG1 expression was positively correlated with LINC00342 (r = 0.453, $P = 3.43 \times 10^{-5}$), MEG3 (r = 0.331, $P = 0.011$) and miR-126-3p (r = 0.282, $P = 0.012$). MALAT1 expression in PBMCs correlated positively with LINC00342 (r = 0.59, $P = 7.35 \times 10^{-8}$) and the protein-coding genes *PTEN* (r = 0.464, $P = 8.68 \times 10^{-5}$) and *FOXO3* (r = 0.283, $P = 0.022$). Conversely, MALAT1 expression was negatively correlated with miR-126-3p (r = − 0.327, $P = 0.0053$), miR-200a-3p (r = − 0.259, $P = 0.0292$), and miR-18a-5p (r = − 0.381, $P = 0.001$) (Supplementary Table 1). Positive correlations were also identified between *FOXO3* expression in PBMCs and the protein-coding genes *PTEN* (r = 0.558, $P = 1.09 \times 10^{-7}$), TGFB2 (r = 0.457, $P = 0.0003$), and *KEAP1* (r = 0.395, $P = 0.0003$). In contrast, *FOXO3* expression was negatively correlated with the ncRNAs H19 (r = − 0.313, $P = 0.009$), TP53TG1 (r = − 0.248, $P = 0.038$), and miR-126-3p (r = − 0.268 $P = 0.02$). Additionally, *PTEN* expression in PBMCs correlated positively with LINC00342 (r = 0.277, $P = 0.22$) and negatively with miR-126-3p (r = − 0.281 $P = 0.013$) and miR-18a-5p (r = − 0.317, $P = 0.005$). Notably, the expression levels of all studied miRNAs in PBMCs showed positive correlations with each other (Supplementary Table 11).

In lung tissue, the relative expression level of H19 showed a positive correlation with TP53TG1 (r = 0.35, $P = 0.027$) and LINC00342 (r = 0.339, $P = 0.026$)

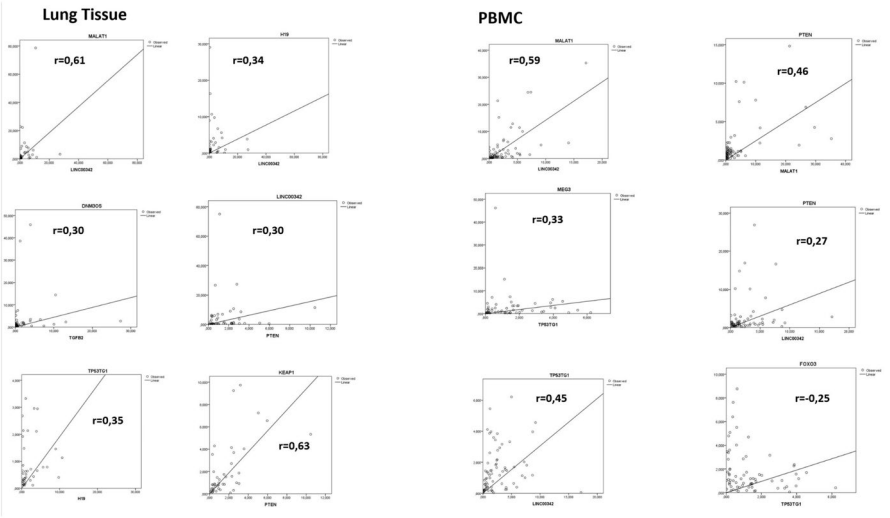

Fig. 9 Correlation between relative expression level of studied lncRNAs, miRNAs, and mRNAs in PBMC and lung tissue (the most significant results are presented). Correlation were analyzed using Spearman correlation coefficient, data are presented in Supplementary Tables 11 and 12

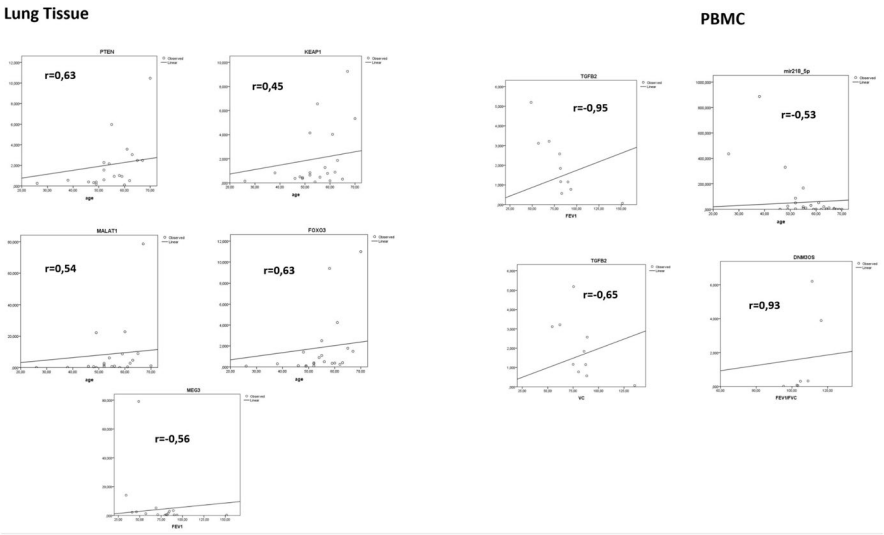

Fig. 10 Correlation expression levels of studied lncRNAs, miRNAs, and mRNAs in PBMCs and lung tissue and clinical/demographic parameters (significant results are presented). Correlations were analyzed using the Spearman correlation coefficient, data are presented in Supplementary Tables 13 and 14

(Supplementary Table 12). LINC00342 expression was positively correlated with MALAT1 (r = 0.553, $P = 1.53 \times 10^{-5}$) and the protein-coding gene *PTEN* (r = 0.305, $P = 0.039$). *TGFB2* expression in lung tissue was positively correlated with *PTEN* (r = 0.441, $P = 0.002$), *FOXO3* (r = 0.598, $P = 1.12 \times 10–5$), and DNM3OS (r = 0.298, $P = 0.043$), while showing a negative correlation with miR-200a-3p (r = − 0.365, $P = 0.013$). *KEAP1* expression was positively correlated with *FOXO3* (r = 0.477, $P = 0.001$) and *PTEN* (r = 0.627, $P = 5.05 \times 10^{-6}$), and a strong positive correlation was found between *FOXO3* and *PTEN* (r = 0.74, $P = 3.66 \times 10^{-9}$). MALAT1 expression was negatively correlated with miR-18a-5p (r = − 0.346, $P = 0.022$) and miR-29a-3p (r = − 0.316, $P = 0.039$). The expression of MEG3 was negatively correlated with miR-126-3p (r = − 0.453, $P = 0.0022$) and miR-29a-3p (r = − 0.377, $P = 0.013$). Strong positive correlations were observed among the expression levels of miR-218-5p, miR-126-3p and miR-18a-5p in lung tissue (Supplementary Table 12).

Correlations between the expression levels of the studied lncRNAs, miRNAs, and mRNAs with clinical/demographic parameters (age, pack/years, FEV1/FVC, VC, FEV1) were analyzed. A negative correlation was observed between patient age and miR-218-5p expression in PBMCs (r = − 0.531, $P = 0.004$). H19 expression in PBMCs was negatively correlated with pack/years (r = − 0.645 $P = 0.011$). DNM3OS expression in PBMCs showed a positive correlation with FEV1/FVC ratio (r = 0.928 $P = 0.007$), while TGFB2 expression was negatively correlated with VC (r = − 0.648, $P = 0.048$) and FEV1 (r = − 0.952, $P = 0.0001$) (Supplementary Table 13).

In lung tissue, the relative expression levels of MALAT1 (r = 0.537, $P = 0.012$), *PTEN* (r = 0.625, $P = 0.002$), *FOXO3* (r = 0.628, $P = 0.002$), and *KEAP1* (r = 0.45,

$P = 0.04$) were positively correlated with patient age. Conversely, MEG3 expression in lung tissue was negatively correlated with FEV1 (r = − 0.565, $P = 0.024$) (Supplementary Table 14). The correlations between gene expression levels, lung function parameters, and patient age suggest a potential role in in lung tissue senescence and the development of fibrotic alterations. However, further validation in larger cohorts and functional studies is required to confirm these findings.

Prognostic Significance of Differentially Expressed lncRNAs, miRNAs and mRNAs in IPF

The diagnostic power of differentially expressed lncRNAs, mRNAs, and miRNAs in IPF was evaluated through receiver operating characteristic (ROC) curve analysis, comparing the area under the curve (AUC) values. Supplementary Fig. 9. illustrates the predictive performance of these biomarkers in PBMCs and lung tissue samples, highlighting their expression profiles' ability to differentiate IPF patients from controls.

TP53TG1 exhibited predictive ability for IPF, with an AUC of 0.7117 (95% CI 0.5944 – 0.8290, $P = 0.002$, cut off = 1.143, sensitivity = 79.2%, specificity = 59.7%) in PBMCs samples and an AUC of 0.6926 (95% CI 0.5324–0.8529, $P = 0.0306$, cut off = 0.651, sensitivity = 72.7%, specificity = 57.1%) in lung tissue samples. MALAT1 demonstrated strong predictive power in PBMCs, achieving an AUC of 0.8140 (95% CI 0.7005–0.9276, $P = 0.0001$, cut off = 1.531, sensitivity = 90.0%, specificity = 64.9%). LINC00342 showed moderate predictive ability in PBMCs, with an AUC of 0.6456 (95% CI 0.5122–0.7791, $P = 0.04$, cut off = 1.452, sensitivity = 77.3%, specificity = 52.5%). Similarly, *PTEN* expression in PBMCs exhibited moderate predictive capability for IPF, with an AUC of 0.7114 (95% CI 0.5568 – 0.8661, $P = 0.004$, cut off = 1.824, sensitivity = 66.7%, specificity = 76.2%). *FOXO3* in PBMCs differentiated IPF patients from controls with an AUC of 0.7407 (95% CI 0.6105 – 0.8709, $P = 0.001$, cut off = 2.482, sensitivity = 57.9%, specificity = 80.9%). In lung tissue, DNM3OS demonstrated moderate predictive power for IPF, with an AUC of 0.6636 (95% CI 0.5057 – 0.8216, $P = 0.05$, cut off = 1.34, sensitivity = 60.0%, specificity = 77.3%). Additionally, several miRNAs in PBMCs showed moderate diagnostic accuracy for IPF. For miR-216-3p, the AUC was 0.6786 (95% CI 0.5754– 0.7817, $P = 0.004$, cut off = 0.6245, sensitivity = 75.0%, specificity = 61.4%). For miR-200a-3p, the AUC was 0.6665 (95% CI 0.5566–0.7764, $P = 0.007$, cut off = 0.6245, sensitivity = 65.6%, specificity = 70.0%). For miR-18a-5p, the AUC was 0.6746 (95% CI 0.5674–0.7817, $P = 0.005$, cut off = 0.5953, sensitivity = 71.9%, specificity = 60.0%).

The diagnostic capability of combined lncRNAs, miRNA, and mRNA for IPF was evaluated through multiple regression analysis followed by ROC analysis. Two informative prognostic models for distinguishing IPF patients from controls were identified, as summarized in Table 4. The first model, which combined TP53TG1, MALAT1, and *PTEN* expression, demonstrated an AUC of 0.928 (95% CI 0.866–0.990, $P = 6 \times 10^{-7}$, sensitivity − 53.3%, specificity − 93.9%) (Fig. 11a). This model exhibited a moderate level of sensitivity but high specificity. The

Table 4 Results of multiple regression analysis of combined evaluation of TP53TG1, MALAT1, PTEN, miR-126-3p gene expressions in PBMCs for discrimination between the IPF and control group

Variables	b	P_{Wald}	OR	95% CI_{OR}
Model 1				
PTEN	0.449	0.04	1.566	1.19–2.47
TP53TG1	− 2.713	0.029	0.066	0.01–0.76
MALAT1	0.164	0.039	1.178	1.01–1.38
Intercept	− 0.994	0.0120	0.370	
$\chi^2 = 35.05$, df = 3, $P = 1.22 \times 10^{-7}$ AUC = 0.928 (95% CI 0.866 -0.990), $P_{ROC} = 6 \times 10^{-7}$ Sensitivity—53.3%, Specificity—93.9%				
Model 2				
miR-126-3p	− 1.377	0.02	0.252	0.05–0.76
TP53TG1	− 4.113	0.032	0.016	0.08–0.71
MALAT1	0.285	0.04	1.330	1.03–1.81
PTEN	0.528	0.048	1.696	1.41–2.86
Intercept	− 0.048	0.0153	0.953	
$\chi^2 = 44.56$, df = 4, $P = 1.77 \times 10^{-8}$ AUC = 0.971 (95% CI 0.935—1.00), $P_{ROC} = 6 \times 10^{-8}$, Sensitivity = 80.0%, Specificity = 95.5%				

b—The beta coefficient for variable, P_{Wald}—the significance for Wald statistics, the OR—(exp (b)), $\chi 2$- the likelihood ratio test (LR), df—the number of degrees of freedom, P—the value for the likelihood ratio test, AUC—area under the curve, 95% CI—95% confidence interval for AUC, P_{ROC}—is the significance for ROC-curve

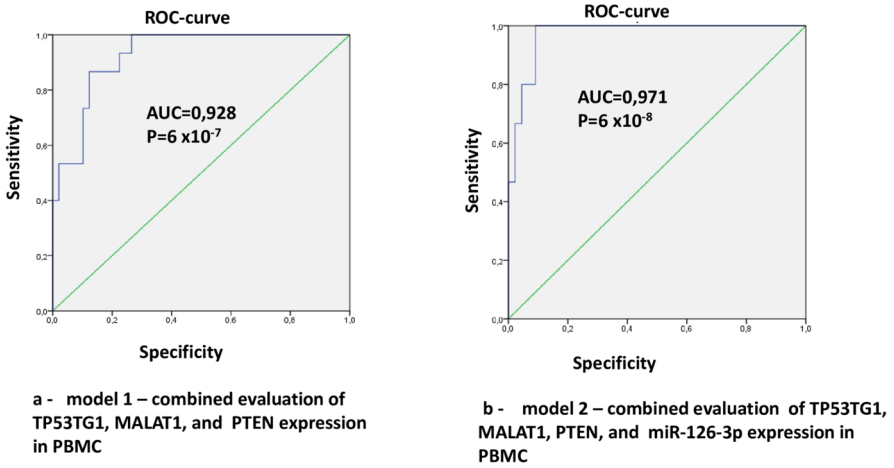

a - model 1 – combined evaluation of TP53TG1, MALAT1, and PTEN expression in PBMC

b - model 2 – combined evaluation of TP53TG1, MALAT1, PTEN, and miR-126-3p expression in PBMC

Fig. 11 The receiver operating characteristic (ROC) curves for results of multiple regression analysis of combined evaluation of TP53TG1, MALAT1, PTEN, and miR-126-3p gene expressions in PBMCs for discrimination between the IPF and control group. The area under the curve (AUC) of Model 1 (**a**), including combined evaluation of TP53TG1 + MALAT1 + PTEN expression in PBMCs can differentiate the IPF patients from the control group with an AUC of 0.928 (95% CI 0.866–0.990, $P = 6 \times 10^{-7}$, sensitivity = 53.3%, specificity = 93.9%). The AUC for Model 2 (**b**), including combined evaluation of TP53TG1 + MALAT1 + PTEN + miR-126-3p expression in PBMCs, was 0.971 (95% CI 0.935–1.00, $P = 6 \times 10^{-8}$, sensitivity = 80.0%, specificity = 95.5%)

second model, which incorporated TP53TG1, MALAT1, *PTEN*, and miR-126-3p expression in PBMCs, showed superior diagnostic performance with an AUC of 0.971 (95% CI 0.935–1.00, $P = 6 \times 10^{-8}$, sensitivity = 80.0%, specificity = 95.5%) (Fig. 11b). This model demonstrated both high sensitivity and specificity, making it a robust classifier for differentiating IPF patients from healthy individuals. These findings suggest that the combined evaluation of multiple gene expression, including lncRNAs, miRNA, and target mRNA, offers a highly sensitive and specific prognostic model for IPF diagnosis. However, validation on independent, larger sample sets is necessary to confirm these results and establish their clinical utility.

Discussion

PF is a condition marked by irreversible remodeling of the pulmonary interstitial tissue, leading to respiratory dysfunction (Giacomelli et al. 2021; Podolanczuk et al. 2013). Among idiopathic interstitial pneumonia-related diseases, IPF stands out as the most prevalent, with the highest incidence and poorest prognosis, characterized by a median survival of 2–4 years post-diagnosis (Giacomelli et al. 2021). The World Health Organization has highlighted a significant increase in PF cases during the COVID-19 pandemic (Tanni et al. 2021). Despite its clinical significance, the underlying mechanisms driving IPF and its rapid progression remain largely undefined. In recent years, the potential role of ncRNAs in uncovering novel therapeutic strategies and identifying biomarkers for complex diseases has garnered considerable attention (Romero et al. 2016; Poulet et al. 2020; Yan et al. 2017). In this study, we focused on specific lncRNAs (TP53TG1, LINC00342, H19, MALAT1, DNM3OS, MEG3), miRNAs (miR-218-5p, miR-126-3p, miR-200a-3p, miR-18a-5p, miR-29a-3p), and target protein-coding genes (*PTEN, TGFB2, FOXO3, KEAP1*). These molecules regulate key signaling pathways, including PI3K/AKT/mTOR, focal adhesion, FoxO, Wnt, and TGF-β/SMAD3, which are implicated in apoptosis, cellular senescence, and EMT.

This study revealed a significant increase in the relative expression level of MALAT1 in PBMCs of IPF patients. However, in lung tissue, no statistically significant differences were observed in MALAT1 expression levels between patients and controls, despite a trend of upregulation. This discrepancy may reflect tissue-specific patterns of MALAT1. A positive correlation was established between MALAT1 and LINC00342 expression both in PBMCs and lung tissue, as well as between MALAT1 and the protein-coding genes *PTEN* and *FOXO3* in PBMCs. Conversely, MALAT1 expression in PBMCs showed a negative correlation with miR-126-3p, miR-200a-3p, and miR-18a-5p. The lncRNA–miRNA and miRNA–mRNA interaction network analysis (Table 2, Figs. 1 and 2) underscored MALAT1's pivotal role in regulating genes associated with key pathways such as TGF-β1/SMAD, PI3K/AKT/mTOR, focal adhesion, and FoxO. These pathways influence processes like EMT, inflammation in lung tissue, apoptosis, and fibrosis. ROC-curve analysis demonstrated that assessing MALAT1 expression in PBMCs offers strong predictive power for distinguishing IPF patients from healthy individuals. This highlights its potential utility as a biomarker.

The role of MALAT1 in fibrosis across various organs is an area of active investigation. A meta-analysis by Ghafouri-Fard et al. (2021) reported that MALAT1 promotes cardiac fibrosis through the miR-141/NLRP3/TGF-β1/Smad2/3 signaling pathway (Ghafouri-Fard et al. 2021). Similarly, it exacerbates renal fibrosis and EMT under hyperglycemia via the miR-145/focal adhesion kinase (FAK) and miR-145/ZEB2 pathways (Ghafouri-Fard et al. 2021). In liver fibrosis, MALAT1 inhibits miR-181a-5p, activating TLR4/NF-κB signaling pathway (Wang et al. 2021).

In lung diseases, MALAT1 expression increases in lipopolysaccharide (LPS)-treated macrophages associated with PF. Knockdown of MALAT1 suppresses C-type lectin domain family 16, member A (Clec16a), reduces pro-inflammatory macrophage activation and cytokine levels, and limits neutrophil infiltration, interstitial thickening, and lung inflammation (Yan et al. 2017; Lai et al. 2022). Cui et al. (2019) demonstrated that MALAT1 knockdown reduced LPS-induced M1 macrophage activation while enhancing alternative M2 macrophage activation, which promotes fibrosis. In mouse models, MALAT1 knockdown reduced LPS-induced inflammation and lung damage while exacerbating subsequent PF (Cui et al. 2019). Further supporting its relevance in IPF, Wang et al. (2020) reported significant upregulation of MALAT1 expression in the peripheral blood of IPF patients (Wang et al. 2020). Lin et al. (2019) showed that MALAT1 acts as a competing endogenous RNA (ceRNA) for miR-150, activating AKT signaling (Lin et al. 2019).

MALAT1's pro-oncogenic effects extend beyond fibrosis through its interactions with miRNA and signaling pathways. For instance, MALAT1 modulates the CDC42/ZEB2 pathway in breast cancer via miR-1/miR-204 inhibition, the TGFA pathway in osteosarcoma via miR376A, the Gli2 pathway in gastric cancer via miR-202, and the IASPP/PHF19 pathway in ovarian cancer via miR-506/miR-211 (Li et al. 2018b). Additionally, it interacts with miR-124 and regulates the RBG2 pathway in cervical cancer, while also modulating miR-200 family (miR-200a-3p, miR-200b-3p, miR-200c-3p), acting as ceRNA (Chen et al. 2019b).

In SARS-CoV-2-related inflammation, MALAT1 interacts with the miR-200 family, impacting TGF-β1/Smad2/3 signaling and ACE2 expression, further linking it to pulmonary and systemic fibrosis pathways (Sodagar et al. 2022). These findings confirm MALAT1's critical role in IPF pathogenesis, reinforcing its importance in fibrosis and inflammation regulation.

A negative correlation was observed between MALAT1 and miR-200a-3p expression levels in PBMCs of IPF patients, where miR-200a-3p was significantly downregulated. Interaction network analysis (Table 2, Fig. 1) revealed that miR-200a-3p interacts with the lncRNAs MALAT1 and H19, as well as with protein-coding genes such as *PTEN, TGFB2,* and *KEAP1*. MirPath analysis (Supplementary Table 1, 2, Fig. 3, 4) identified a wide array of miR-200a-3p target genes involved in several pathways, including the FoxO-signaling pathway ($P = 3.8806e^{-06}$), PI3K/AKT-signaling pathway ($P = 3.599e^{-05}$), cell cycle regulation ($P = 1.1632e^{-07}$), cellular senescence ($P = 0.00018937$), mTOR-signaling pathway ($P = 0.00080421$), Wnt-signaling pathway ($P = 0.00153709$), and focal adhesion ($P = 2.969e^{-09}$).

The miR-200 family, comprising miR-200a, miR-200b, miR-200c, miR-141, and miR-429, is encoded by two genomic clusters located at 1p36.33 (miR-200b/200a/429) and 12p13.31 (miR-200c/141) (Klicka et al. 2022). These miRNAs

have been implicated in IPF and various cancers, largely due to their regulation of cell cycle pathways and inhibition of EMT (Klicka et al. 2022; Moimas et al. 2019). Previous studies have consistently reported downregulation of the miR-200 family in IPF (Yang et al. 2012a, b). The specific contribution of miR-200a to IPF development is a focus of ongoing research. Mansour et al. (2021) demonstrated that in a rat model of bleomycin-induced PF treated with tadalafil, miR-200a levels were upregulated and inversely correlated with key pro-fibrotic pathway components, including TGF-β/ SMAD3/α-SMA, Snail, and p-AKT/p-FOXO3a, as well as α-SMA levels (Mansour et al. 2021). Similarly, Kadota et al. (2021) highlighted miR-200a's role in suppressing TGF-β- and WNT-signaling pathways, inhibiting myofibroblast differentiation and lung epithelial cell senescence (Kadota et al. 2021). Moimas et al. (2019) laid important groundwork by demonstrating a marked downregulation of the miR-200 family in alveolar type II cells from IPF patients (Moimas et al. 2019). This was accompanied by upregulation of EMT markers (ZEB1, ZEB2) and cellular senescence markers (CDKN1A and CDKN2A) (Moimas et al. 2019).

In the present study, we observed downregulation of miR-126-3p in PBMCs of IPF patients. Network interaction analysis of lncRNAs, miRNAs, and mRNAs (Table 2, Fig. 1) revealed interactions between miR-126-3p and the protein-coding gene *FOXO3*. According to MirPath analysis, miR-126-3p is involved in the regulation of several key pathways, including PI3K/AKT-signaling pathway ($P = 0.000499$), FoxO-signaling pathway ($P = 3.480e^{-05}$), cellular senescence ($P = 0.000795$), and apoptosis ($P = 0.00242$) (Supplementary Table 1, 2, Fig. 3, 4). The role of miR-126-3p in fibrosis development has been demonstrated previously. In a rat PF model and a human bronchial epithelial cell line (16HBE) treated by carbon black particles, miR-126 reduction was associated with activation of PI3K/AKT/mTOR-signaling pathway (Han et al. 2020). Similarly, Jordan et al. (2021) reported that miR-126-3p downregulation occurs in cardiac and kidney fibrosis, while upregulation of miR-126-3p reduces EndMT (Jordan et al. 2021). In myocardial fibrosis, reduced miR-126 expression lead to activation of the PI3K/AKT-signaling pathway (Li et al. 2021).

In this study, we also found that miR-18a-5p is downregulated in PBMCs of IPF patients. Negative correlations were observed between miR-18a-5p expression levels and MALAT1 and *PTEN* in PBMCs, as well as MALAT1 and LINC00342 in lung tissue. Network analysis revealed that miR-18a-5p regulates apoptosis and EMT, with several target mRNAs identified, including *FOXO3* and *PTEN*. Interactions with lncRNAs such as H19 and TP53TG1 were also detected (Table 2, Fig. 1). MirPath analysis highlighted miR-18a-5p involvement in regulating multiple pathways, including PI3K/AKT-signaling pathway ($P = 1.8622e^{-09}$), focal adhesion ($P = 2.969e^{-09}$), FoxO-signaling pathway ($P = 3.8806e^{-06}$), cell cycle ($P = 0.00014$), and cellular senescence ($P = 0.0000691$) (Supplementary Table 1, 2, Fig. 3, 4). Several lncRNA, such as GAS5, TP53TG1, FENDRR, and CASC2, act as molecular sponges for miR-18a-5p (Kolenda et al. 2020; Xiao et al. 2018). Overall, miR-18a is involved in regulating cell cycle, proliferation, apoptosis, autophagy, and stress responses (Kolenda et al. 2020). While miR-18a expression is upregulated in various cancers (Shen et al. 2019), its expression is reduced in PF. miR-18a knockdown has been shown to increase synthesis of pro-fibrotic proteins such as collagen 1,

fibronectin (FN1), α-SMA, as well as enhance fibroblast proliferation and migration (Li et al. 2018a, b). The antifibrotic effects of miR-18a are primarily mediated through its inhibition of TGFBR2, suppressing the TGF-β/SMAD2/3 signaling pathway (Zhang et al. 2017a, b).

Aberrant expression of miRNAs—either upregulation or downregulation—is a key mechanism underlying the pathogenesis of various diseases, including PF (Seyhan 2024; Mehjabin et al. 2023). Consequently, extensive research, preclinical studies, and clinical trials are being conducted to evaluate the therapeutic potential of miRNA mimics and inhibitors as pivotal tools for disease treatment. The miRNA-based therapies can inhibit target genes and modulate specific signaling pathways (Kp et al. 2024; Braicu et al. 2013; Seyhan 2024; Usman Pp and Sekar 2024; Mehjabin et al. 2023). Notably, the preclinical development of MGN-4220, a therapeutic molecule targeting miR-29 for cardiac fibrosis treatment, has been reported by Miragen Therapeutics (Seyhan 2024).

In this study, TP53TG1 lncRNA expression was significantly downregulated both in PBMCs and lung tissue samples from IPF patients. ROC analysis revealed that TP53TG1 expression in PBMCs and lung tissue has moderate predictive power for distinguishing IPF patients from healthy controls. Correlation analysis indicated a positive correlation between TP53TG1 and MEG3, LINC00342, and miR-126-3p in PBMCs, as well as with H19 in lung tissue, while a negative correlation with *FOXO3* was observed in PBMCs. LncRNA- miRNA and miRNA-mRNA interaction network analysis (Table 2) revealed that TP53TG1 acts as a pro-apoptotic factor in lung cells, regulating the miR-18a-5p/PTEN axis (Chen et al. 2021a; Xiao et al. 2018). Furthermore, TP53TG1 is implicated as a regulator of actin alpha 2, smooth muscle (ACTA2), fibronectin 1 (FN1), and various collagens (Collagen 1α1, 3α, and I), functioning as an antifibrotic factor (Sun et al. 2022). Increased TP53TG1 expression has been shown to reduce bleomycin-induced experimental PF in mice (Sun et al. 2022). Published evidence also suggests that TP53TG1 functions as a tumor suppressor. It inhibits hepatocellular carcinoma (HCC) progression and liver fibrosis by triggering ubiquitin-dependent degradation of the PRDX4, thereby blocking the WNT/β-catenin signaling pathway (Chen et al. 2021a). Conversely, Lu et al. (2021) demonstrated that increased TP53TG1 expression promoted HCC cell proliferation via ERK1/ERK2 pathway activation (Lu et al. 2021). In breast cancer, TP53TG1 exerts tumor-suppressive effects by binding to YBX2, suppressing the PI3K/AKT-signaling pathway (Shao et al. 2020). Additionally, TP53TG1 binds to miR-18a, facilitating the synthesis of the anti-tumor enzyme PTEN and promoting apoptosis in non-small cell lung cancer tissues (Yuan et al. 2017). Our findings align with previous studies, demonstrating a significant reduction in TP53TG1 expression in IPF patients, further supporting its critical role in fibrosis regulation.

The present study shows that DNM3OS expression is significantly upregulated in lung tissue samples from IPF patients. A positive correlation between DNM3OS expression in lung tissue and *TGFB2* was observed. Through lncRNA–miRNA and lncRNA–mRNA interaction network analysis (Table 2, Fig. 2), we demonstrate that DNM3OS plays a key role in regulating EMT, pulmonary inflammation, and functions as both pro-fibrotic and anti-apoptotic factor. Dysregulation of the TGF-β signaling pathway is well-established as a critical factor in the pathogenesis of PF

(Gauldie et al. 2007). Moreover, DNM3OS has been shown to regulate both SMAD-mediated (SMAD4, SMAD2, p-SMAD2) and SMAD-independent (p-Akt, Akt, p-GSK-3β, GSK-3β) pathways of TGF-β1-mediated pro-fibrotic signal transduction (Savary et al. 2019). In lung fibroblasts, DNM3OS is fragmented into three miRNAs (miR-199a-5p, miR-199a-3p and miR-214-3p), all of which are linked to the TGF-β signaling pathway (Savary et al. 2019). Specifically, miR-199a-5p inhibits the expression of CAV1 and disrupts the degradation of TGFβ/TGFβR complex, while miR-214-3p regulates COX-2 and GSK-3β expression, thus promoting the fibroblast-to-myofibroblast transition. Additionally, miR-199a-3p regulates the TGFβ-induced inhibition of fibroblast growth factors FGF7 and HGF, thereby inhibiting tissue repair (Savary et al. 2019). Liu et al. (2018) demonstrated that miR-199a is involved in modulating the expression of SIRT1 in alveolar macrophages, influencing pulmonary inflammation in acute respiratory distress syndrome (ARDS) (Liu et al. 2018). Furthermore, DNM3OS has been shown to regulate the interaction between the pro-fibrotic TGF-β and Wnt-signaling pathways (Savary et al. 2019). The role of DNM3OS in cardiac fibroblast activation has also been confirmed. DNM3OS knockdown inhibited the TGF-β1/Smad2/3 pathway and reduced myocardial fibrosis (Kong et al. 2021). Increased expression of DNM3OS is linked to tumor progression via EMT regulation (Wang et al. 2019b).

In the present study, upregulation of LINC00342 was detected in PBMCs of IPF patients. Furthermore, a positive correlation was observed between LINC00342 expression in both PBMCs and lung tissue with MALAT1 and *PTEN*, while a negative correlation with miR-18a-5p was identified. The results of lncRNA–miRNA and mRNA interaction network analysis (Table 2, Fig. 1) suggest that LINC00342 plays a role in regulating EMT and modulating pulmonary inflammation. Su et al. (2022) reported that activation of the miR-15b/TPBG signaling pathway by LINC00342 drives the progression and metastasis of lung adenocarcinoma and induces EMT in A549 cells (Su et al. 2022). Increased expression of LINC00342 in non-small cell lung cancer (NSCLC) tissues has also been established (Wang et al. 2016). This upregulation, along with its binding to miR-203a-3p (Chen et al. 2019c), and suppression of the anti-oncogenic activities of p53 and PTEN proteins (Tang et al. 2019) are key factors driving enhanced proliferation and metastasis in NSCLC. In contrast, Fan and Jian (2020) demonstrated that miR-203a-3p regulates the TGF-β/Smad3 signaling pathway and promotes TGF-β1-induced EMT in asthma (Fan and Jian 2020). Additionally, Liu et al. (2019) detected upregulation of LINC00342 expression in peripheral blood lymphocytes of chronic kidney disease patients (Liu et al. 2019).

Increased expression of *PTEN* in PBMCs was observed in the IPF group. Additionally, a positive correlation between *PTEN* expression in PBMCs and *FOXO3,* as well as a negative correlation with miR-18a-5p and miR-126-3p, was demonstrated. In lung tissue, *PTEN* expression was positively correlated with *TGFB2, FOXO3,* and LINC00342. The miRNA-mRNA interaction network analysis (Table 2, Fig. 1) revealed that *PTEN* is a target for miR-218-5p, miR-200a-3p, miR-18a-5p, and miR-29a-3p, and is involved in the regulation of apoptosis, fibrosis, and EMT. Several studies have shown that miR-19b-3p, miR-23a-3p, and miR-486-5p directly bind to the 3′-untranslated region of *PTEN*, leading to its downregulation and activation of

the PI3K/AKT/mTOR-signaling pathway, as well as inhibition of apoptosis (Zhao and Li 2021; Chen et al. 2022; Gao et al. 2018). Interaction of miR-221-3p and miR-222-3p with *PTEN* resulted in decreased oxidative stress and mitochondrial apoptosis in lung cancer cells (Tepebaşı and Öztürk 2023). Yu et al. (2021) demonstrated that miR-21 binding to *PTEN* modulates the proliferation and migration of airway smooth muscle cells and promotes EMT (Yu et al. 2021). Tao et al. (2019) showed that miR-216a binding to *PTEN* enhances the proliferation and fibrogenesis of human cardiac fibroblasts (Tao et al. 2019). Tian et al. (2019) reported low levels of *PTEN* expression in fibroblasts and epithelial cells from IPF lungs (Tian et al. 2019). The reduced *PTEN* expression in lung tissue from bleomycin-induced IPF mice resulted in increased EMT, Snail, and matrix metalloproteinase levels, along with simultaneous reduction in E-cadherin and laminin-β1 levels, leading to lung tissue damage and fibrosis (Miyoshi et al. 2013). Furthermore, downregulation of *PTEN* in vivo in IPF mice resulted in overexpression of type I collagen and activation of the CTGF/CCN2 pro-fibrotic pathway (Parapuram et al. 2015). PTEN exerts a significant antifibrotic effect; together with caveolin 1 (CAV1), it stabilizes the proliferation of myofibroblasts in fibrotic lung tissue (Xia et al. 2010). The pro-inflammatory potential of PTEN is associated with its ability to directly bind to NLR family pyrin domain containing 3 (NLRP3), leading to dephosphorylation of tyrosine 32, maturation of inflammasomes, and activation of pro-inflammatory cytokines of the IL-1 family (Akbal et al. 2022). The increased expression of *PTEN* in PBMCs from IPF patients observed in our study may be related to the simultaneous downregulation of miR-200a-3p and miR-18a-5p. The increased expression levels of *PTEN* in PBMCs were also observed in patients with coronary artery disease, accompanied by a decrease in miR-21, a microRNA that interacts with *PTEN* (Nariman-Saleh-Fam et al. 2019). Based on multiple regression and ROC analysis, our study determined a highly informative prognostic model for IPF, which includes simultaneous assessment of TP53TG1, MALAT1, *PTEN,* and miR-126-3p expression.

The expression of *FOXO3* was significantly elevated in PBMCs of IPF patients. A positive correlation between *FOXO3* expression level in PBMCs and lung tissue was observed with *PTEN, TGFB2,* and *KEAP1*. The miRNA–mRNA interaction network analysis (Table 2, Fig. 1) revealed that *FOXO3* is a target of miR-218-5p, miR-126-3p, miR-18a-5p, and miR-29a-3p, and plays a role in regulating apoptosis, fibrosis, and the modulation of EMT. Al-Tamari et al. (2018) demonstrated that FOXO3 is pivotal in regulating signaling pathways associated with fibrogenesis (Al-Tamari et al. 2018). Li et al. (2023) showed that FOXO3 regulates Smad3 and Smad7 through SPON1 circular RNA, thus preventing fibrosis formation (Li et al. 2023). Elevated levels of *FOXO3* enhance the resistance of NSCLC cells to radiation therapy-induced apoptosis by directly interacting with miR-182 (Chen et al. 2019a). Another study revealed that *FOXO3*binding to miR-217 contributes to enhanced survival of endothelial cell under hyperglycaemic conditions (Cheng et al. 2020). It has also been shown that miR-29b-3p suppresses endotoxin-induced cardiomyocyte apoptosis by binding to *FOXO3* (Li et al. 2020). Furthermore, the interaction of *FOXO3* with miR-23a results in a significant reduction of proliferative capacity and cell cycle arrest of lung fibroblast cells (Wang et al. 2024). In contrast, Zhou et al. (2020) overexpression of miR-96 or suppression of *FOXO3* leads to partial

regression of carbon nanoparticle-induced fibrosis through inhibition of the NLRP3 inflammasome (Zhou et al. 2020). Zhong et al. (2023) reported that increased expression of *FOXO3* in tumor tissue is associated with poor prognosis in gastric cancer, while elevated expression of miR-18a-5p, which interacts with *FOXO3,* was linked to better prognosis in patients with gastric cancer (Zhong et al. 2023).

Pathway enrichment analysis revealed the most enriched signaling pathway targeted by the investigated lncRNAs and miRNAs. As shown in the hierarchical pathway correlation clustering tree (Figs. 3, 4, Supplementary Figs. 1, 2, 4), the most prominent clusters included the focal adhesion and PI3K-Akt signaling pathways. Other enriched pathways included Wnt-signaling, apoptosis, FoxO-signaling, mTOR-signaling, and cellular senescence pathways.

Published studies confirm the involvement of focal adhesion and PI3K/AKT pathways in the development of IPF. PI3K/AKT/mTOR-signaling pathway is activated by various growth factors and regulates processes such as cell proliferation, adhesion, migration, invasion, metabolism, survival, apoptosis, autophagy, and cellular senescence (Ersahin et al. 2015; Saxton and Sabatini 2017; Biray Avci et al. 2020). Dysregulation of the PI3K/AKT/mTOR pathway has been linked to PF (Gui et al. 2018; Yue et al. 2024). Key molecules within this pathway mediate cell survival and proliferation by inhibiting apoptosis (Saxton and Sabatini 2017). Moreover, overexpression of α-SMA and TGF-β in lung fibrosis has been associated with activation of the PI3K/AKT-signaling cascade (Wang et al. 2021). This cascade interacts with several other signaling pathways, including TGF-β1/Smad3/α-SMA, Wnt/β-catenin, and FAK, all of which are closely related to the pathogenesis of lung fibrosis (Rosenbloom et al. 2013; Wang et al. 2021).

Focal adhesions are multi-protein complexes that connect the cytoskeleton to the extracellular matrix, playing a critical role in cell adhesion and function (Schumacher et al. 2022). These complexes include molecules such as FAK, integrins, fibronectin, vitronectin, and collagen (Casarella et al. 2024). Focal adhesion signaling molecules are essential for cell adhesion, migration, and transmitting signals that affect cell survival and differentiation (Schumacher et al. 2022; Casarella et al. 2024). The focal adhesion pathway is initiated by the activation of integrins, leading to the activation of FAK and subsequent downstream cascades, including the PI3K/AKT pathway (Lin et al. 2022). FAK activation enhances fibroblast responses to the pro-fibrotic factor TGF-β (Wheaton et al. 2017). Several studies have demonstrated cross-activation between the TGF-β and FAK signaling pathways in fibrosis (Leask 2013). The activation of integrins and FAK plays a significant role in lung tissue damage and the activation of fibrogenesis in IPF (Wheaton et al. 2017).

The increased incidence of lung cancer among IPF patients may be linked to the activation of common signaling pathways associated with carcinogenesis, such as PI3K/AKT/ mTOR, focal adhesion and the cross-talk between PI3K/AKT and FAK signaling cascades (Podolanczuk et al. 2013; Lin et al. 2022; Yue et al. 2024). Given the pivotal role of the PI3K/AKT and FAK pathways in the pathogenesis of IPF, targeted therapies that inhibit PI3K/AKT and FAK activity (e.g., PI3K/AKT inhibitors and tyrosine kinase receptor inhibitors) may offer a novel therapeutic approach for treating IPF (Wang et al. 2022). For example, Pan et al. (2023) demonstrated that Nintedanib, a triple tyrosine kinase receptor inhibitor, regulates the PI3K/AKT/

mTOR pathway, leading to decreased inflammation and reduced fibrotic changes in bleomycin-induced PF (Pan et al. 2023). Similarly, Chen et al. 2023 showed that inhibition of the FAK signaling pathway reduces EndoMT and suppresses the NLRP3 inflammasome, thereby alleviating lung inflammation and fibrosis (Chen et al. 2023). Yu et al (2022) revealed that Nintedanib inhibits EndoMT by modulating FAK activity (Yu et al. 2022).

This study has several limitations. The sample size was small, primarily due to the rarity of IPF, with a prevalence of only 8–12 cases per 100,000 people in our region and a survival rate of 2–5 years (Richeldi et al. 2015). Moreover, the specific nature of IPF limits the eligibility of patients for invasive procedures, such as lung biopsies, to obtain tissue samples. Our study included only patients with a first-time IPF diagnosis, who had not previously undergone antifibrotic therapy and for whom lung biopsies were available. Consequently, larger and independent patient cohorts are required to validate our findings on altered gene expression. Another limitation is the potential clinical heterogeneity of IPF and the presence of comorbidities in our patient population, which may have influenced the results. Additionally, as our study focused on newly diagnosed IPF patients, we were unable to evaluate variability in disease progression rates. This will be addressed in our upcoming long-term follow-up studies.

In this study, we have characterized the differential expression of lncRNAs, miRNAs, and their target mRNAs in the PBMCs and lung tissue of IPF patients. Specifically, we observed the differential expression of lncRNAs (MALAT1, TP53TG1, LINC00342), miRNAs (miR-126-3p, miR-200a-3p, miR-18a-5p), and target protein-coding genes (*FOXO3* and *PTEN*) in PBMCs of IPF patients. In contrast, significant changes in gene expression in lung tissue were confirmed only for the lncRNAs TP53TG1 and DNM3OS, which may be attributed to tissue and cell-specific differences in ncRNA and mRNA expression, as well as the pathological features of IPF. Numerous studies have shown that the expression profiles of mRNAs and ncRNAs vary across different tissues and cell types. Moreover, published data indicate that lncRNAs expression is more tissue-specific compared to protein-coding genes (Zhu et al. 2016; Derrien et al. 2012).

The observed correlation between the expression levels of some genes and clinical parameters such as lung function and patient age suggests their potential role in lung tissue senescence and fibrotic changes. However, these findings require further validation through larger sample sizes and functional studies. Multiple regression and ROC curve analysis revealed a high predictive power for a combined assessment of lncRNAs TP53TG1 and MALAT1, miRNA miR-126-3p, and mRNA *PTEN* expression levels in PBMCs, with an AUC of 0.971, sensitivity = 80.0%, specificity = 95.5%, $P = 6 \times 10^{-8}$, for distinguishing IPF patients from healthy individuals. However, these results necessitate validation in independent cohorts. Further functional validation studies are required to elucidate the specific molecular mechanisms by which the studied lncRNAs, miRNAs, and their targets contribute to the pathogenesis of IPF.

Supplementary Information The online version contains supplementary material available at https://doi.org/10.1007/s10528-024-11012-z.

Acknowledgements We sincerely thank all patients and healthy volunteers for their invaluable participation.

Author Contributions Gulnaz F. Korytina: Conceptualization, Validation, Formal analysis, Investigation, Visualization, Writing—Original Draft, Writing—Review & Editing, Project administration. Vitaly A. Markelov: Methodology, Software, Validation, Formal analysis, Investigation, Visualization, Writing—Original Draft. Irshat A. Gibadullin: Resources, Methodology, Data Curation, Writing—Original Draft. Shamil R. Zulkarneev: Methodology, Investigation, Visualization, Software, Writing—Original Draft. Timur R. Nasibullin: Software, Formal analysis, Writing—Original Draft. Rustem H. Zulkarneev: Resources, Data Curation¸ Writing—Original Draft, Writing—Review & Editing. Arthur M. Avzaletdinov: Resources, Methodology, Data Curation, Writing—Original Draft, Writing—Review & Editing. Sergey N. Avdeev: Conceptualization, Writing—Review & Editing. Naufal Sh. Zagidullin: Conceptualization, Visualization, Writing—Original Draft, Writing—Review & Editing, Supervision, Project administration, Funding acquisition.

Funding This work was supported by the Bashkir State Medical University Strategic Academic Leadership Program (PRIORITY-2030).

Data Availability The datasets generated during and/or analysed during the current study are available from the corresponding author on reasonable request.

Declarations

Competing interest The authors declare no competing interests.

Ethical Approval Study was approved by the Ethics Committee of the Bashkir State Medical University (21.09.2022, №3). All procedures involving human participants were conducted in compliance with the Ethical Standards of the Institutional and/or National Research Ethics Committee and the 1964 Helsinki Declaration and its subsequent amendments, or comparable ethical guidelines.

Consent to Participate Written informed voluntary consent was obtained from all participants involved in the study.

References

Akbal A, Dernst A, Lovotti M et al (2022) How location and cellular signaling combine to activate the NLRP3 inflammasome. Cell Mol Immunol 19(11):1201–1214. https://doi.org/10.1038/s41423-022-00922-w

Ali MS, Singh J, Alam MT et al (2022) Non-coding RNA in idiopathic interstitial pneumonia and Covid-19 pulmonary fibrosis. Mol Biol Rep 49(12):11535–11546. https://doi.org/10.1007/s11033-022-07820-4

Allen RJ, Guillen-Guio B, Oldham JM et al (2020) Genome-wide association study of susceptibility to idiopathic pulmonary fibrosis. Am J Respir Crit Care Med 201(5):564–574. https://doi.org/10.1164/rccm.201905-1017OC

Al-Rugeebah A, Alanazi M, Parine NR (2019) MEG3: an oncogenic long non-coding RNA in different cancers. Pathol Oncol Res 25(3):859–874. https://doi.org/10.1007/s12253-019-00614-3

Al-Tamari HM, Dabral S, Schmall A et al (2018) FoxO3 an important player in fibrogenesis and therapeutic target for idiopathic pulmonary fibrosis. EMBO Mol Med 10(2):276–293. https://doi.org/10.15252/emmm.201606261

Bellezza I, Giambanco I, Minelli A, Donato R (2018) Nrf2-Keap1 signaling in oxidative and reductive stress. Biochim Biophys Acta Mol Cell Res 5:721–733. https://doi.org/10.1016/j.bbamcr.2018.02.010

Biray Avci C, Sezgin B, Goker Bagca B et al (2020) PI3K/AKT/mTOR pathway and autophagy regulator genes in paranasal squamous cell carcinoma metastasis. Mol Biol Rep 47(5):3641–3651. https://doi.org/10.1007/s11033-020-05458-8

Boateng E, Krauss-Etschmann S (2020) miRNAs in lung development and diseases. Int J Mol Sci 21(8):2765. https://doi.org/10.3390/ijms21082765

Braicu C, Calin GA, Berindan-Neagoe I (2013) MicroRNAs and cancer therapy—from bystanders to major players. Curr Med Chem 20(29):3561–3573. https://doi.org/10.2174/09298673113202900002

Cai B, Yang L, Do Jung Y et al (2022) PTEN: an emerging potential target for therapeutic intervention in respiratory diseases. Oxid Med Cell Longev 2022:4512503. https://doi.org/10.1155/2022/4512503

Casarella S, Ferla F, Di Francesco D et al (2024) Focal adhesion's role in cardiomyocytes function: from cardiomyogenesis to mechanotransduction. Cells 8:664. https://doi.org/10.3390/cells13080664

Cavallari I, Ciccarese F, Sharova E et al (2021) The miR-200 family of microRNAs: fine tuners of epithelial-mesenchymal transition and circulating cancer biomarkers. Cancers (Basel) 3(23):5874. https://doi.org/10.3390/cancers13235874

Chen L, Chen R, Kemper S et al (2015) Suppression of fibrogenic signaling in hepatic stellate cells by Twist1-dependent microRNA-214 expression: role of exosomes in horizontal transfer of Twist1. Am J Physiol Gastrointest Liver Physiol 309(6):G491–G499. https://doi.org/10.1152/ajpgi.00140.2015

Chen CY, Chen J, He L, Stiles BL (2018) PTEN: tumor suppressor and metabolic regulator. Front Endocrinol (Lausanne) 9:338. https://doi.org/10.3389/fendo.2018.00338

Chen G, Yu L, Dong H et al (2019a) MiR-182 enhances radioresistance in non-small cell lung cancer cells by regulating FOXO3. Clin Exp Pharmacol Physiol 46(2):137–143. https://doi.org/10.1111/1440-1681.13041(a)

Chen J, Liu X, Xu Y et al (2019b) TFAP2C-activated MALAT1 modulates the chemoresistance of docetaxel-resistant lung adenocarcinoma cells. Mol Ther Nucleic Acids 14:567–582. https://doi.org/10.1016/j.omtn.2019.01.005

Chen QF, Kong JL, Zou SC et al (2019c) LncRNA LINC00342 regulated cell growth and metastasis in non-small cell lung cancer via targeting miR-203a-3p. Eur Rev Med Pharmacol Sci 23(17):7408–7418. https://doi.org/10.26355/eurrev_201909_18849

Chen B, Lan J, Xiao Y et al (2021a) Long noncoding RNA TP53TG1 suppresses the growth and metastasis of hepatocellular carcinoma by regulating the PRDX4/β-catenin pathway. Cancer Lett 513:75–89. https://doi.org/10.1016/j.canlet.2021.04.022

Chen J, Ding C, Yang X, Zhao J (2021b) BMSCs-derived exosomal MiR-126–3p inhibits the viability of NSCLC cells by targeting PTPN9. J BUON 26(5):1832–1841

Chen Y, Yang JL, Xue ZZ et al (2021c) Effects and mechanism of microRNA-218 against lung cancer. Mol Med Rep 23(1):28. https://doi.org/10.3892/mmr.2020.11666

Chen J, Huang T, Liu R et al (2022) Congenital microtia patients: the genetically engineered exosomes released from porous gelatin methacryloyl hydrogel for downstream small RNA profiling, functional modulation of microtia chondrocytes and tissue-engineered ear cartilage regeneration. J Nanobiotechnology 20(1):164. https://doi.org/10.1186/s12951-022-01352-6

Chen WC, Yu WK, Su VY et al (2023) NLRP3 inflammasome activates endothelial-to-mesenchymal transition via focal adhesion kinase pathway in bleomycin-induced pulmonary fibrosis. Int J Mol Sci 24(21):15813.

Cheng L, Wang P, Tian R et al (2019) LncRNA2Target v2.0: a comprehensive database for target genes of lncRNAs in human and mouse. Nucleic Acids Res 47(D1):D140–D144. https://doi.org/10.1093/nar/gky1051

Cheng J, Hu W, Zheng F et al (2020) hsa_circ_0058092 protects against hyperglycemia-induced endothelial progenitor cell damage via miR-217/FOXO3. Int J Mol Med 46(3):1146–1154. https://doi.org/10.3892/ijmm.2020.4664

Cui H, Banerjee S, Guo S et al (2019) Long noncoding RNA Malat1 regulates differential activation of macrophages and response to lung injury. JCI Insight 4(4):e124522. https://doi.org/10.1172/jci.insight.124522

Derrien T, Johnson R, Bussotti G et al (2012) The GENCODE v7 catalog of human long noncoding RNAs: analysis of their gene structure, evolution, and expression. Genome Res 22(9):1775–1789. https://doi.org/10.1101/gr.132159.111

Ebrahimi F, Gopalan V, Smith RA, Lam AK (2014) miR-126 in human cancers: clinical roles and current perspectives. Exp Mol Pathol 96(1):98–107. https://doi.org/10.1016/j.yexmp.2013.12.004

Ersahin T, Tuncbag N, Cetin-Atalay R (2015) The PI3K/AKT/mTOR interactive pathway. Mol Biosyst 11(7):1946–1954. https://doi.org/10.1039/c5mb00101c

Fan Q, Jian Y (2020) MiR-203a-3p regulates TGF-β1-induced epithelial-mesenchymal transition (EMT) in asthma by regulating Smad3 pathway through SIX1. Biosci Rep 40(2):BSR20192645. 10.1042/BSR20192645

Ferrè F, Colantoni A, Helmer-Citterich M (2016) Revealing protein-lncRNA interaction. Brief Bioinform 17(1):106–116. https://doi.org/10.1093/bib/bbv031

Fingerlin TE, Murphy E, Zhang W et al (2013) Genome-wide association study identifies multiple susceptibility loci for pulmonary fibrosis. Nat Genet 45(6):613–20. Erratum in: Nat Genet 45(11):1409. https://doi.org/10.1038/ng.2609

Fraser E, Denney L, Antanaviciute A et al (2021) Multi-modal characterization of monocytes in idiopathic pulmonary fibrosis reveals a primed type I interferon immune phenotype. Front Immunol 12:623430. https://doi.org/10.3389/fimmu.2021.623430

Gao Y, Zhang J, Liu Y et al (2017) Regulation of TERRA on telomeric and mitochondrial functions in IPF pathogenesis. BMC Pulm Med 17(1):163. https://doi.org/10.1186/s12890-017-0516-1

Gao ZJ, Yuan WD, Yuan JQ et al (2018) miR-486-5p functions as an oncogene by targeting PTEN in non-small cell lung cancer. Pathol Res Pract 214(5):700–705. https://doi.org/10.1016/j.prp.2018.03.013

Gauldie J, Bonniaud P, Sime P et al (2007) TGF-beta, Smad3 and the process of progressive fibrosis. Biochem Soc Trans 35(Pt 4):661–664. https://doi.org/10.1042/BST0350661

George PM, Wells AU, Jenkins RG (2020) Pulmonary fibrosis and COVID-19: the potential role for antifibrotic therapy. Lancet Respir Med 8(8):807–815. https://doi.org/10.1016/S2213-2600(20)30225-3

Ghafouri-Fard S, Esmaeili M, Taheri M (2020) H19 lncRNA: roles in tumorigenesis. Biomed Pharmacother 123:109774. https://doi.org/10.1016/j.biopha.2019.109774

Ghafouri-Fard S, Abak A, Talebi SF et al (2021) Role of miRNA and lncRNAs in organ fibrosis and aging. Biomed Pharmacother 143:112132. https://doi.org/10.1016/j.biopha.2021.112132

Giacomelli C, Piccarducci R, Marchetti L, Romei C, Martini C (2021) Pulmonary fibrosis from molecular mechanisms to therapeutic interventions: lessons from post-COVID-19 patients. Biochem Pharmacol 193:114812. https://doi.org/10.1016/j.bcp.2021.114812

Gokey JJ, Snowball J, Sridharan A et al (2018) MEG3 is increased in idiopathic pulmonary fibrosis and regulates epithelial cell differentiation. JCI Insight 3(17):e122490. https://doi.org/10.1172/jci.insight.122490

Goyal B, Yadav SRM, Awasthee N et al (2021) Diagnostic, prognostic, and therapeutic significance of long non-coding RNA MALAT1 in cancer. Biochim Biophys Acta Rev Cancer 1875:188502. https://doi.org/10.1016/j.bbcan.2021.188502

Gui X, Chen H, Cai H et al (2018) Leptin promotes pulmonary fibrosis development by inhibiting autophagy via PI3K/Akt/mTOR pathway. Biochem Biophys Res Commun 498(3):660–666. https://doi.org/10.1016/j.bbrc.2018.03.039

Han B, Chu C, Su X et al (2020) N^6-methyladenosine-dependent primary microRNA-126 processing activated PI3K-AKT-mTOR pathway drove the development of pulmonary fibrosis induced by nanoscale carbon black particles in rats. Nanotoxicology 14(1):1–20. https://doi.org/10.1080/17435390.2019.1661041

Herazo-Maya JD, Noth I, Duncan SR et al (2013) Peripheral blood mononuclear cell gene expression profiles predict poor outcome in idiopathic pulmonary fibrosis. Sci Transl Med 5(205):205ra136. https://doi.org/10.1126/scitranslmed.3005964

Hoffmann J, Machado D, Terrier O et al (2016) Viral and bacterial co-infection in severe pneumonia triggers innate immune responses and specifically enhances IP-10: a translational study. Sci Rep 6:38532. https://doi.org/10.1038/srep38532

Huang HY, Lin YC, Li J et al (2020) miRTarBase 2020: updates to the experimentally validated microRNA-target interaction database. Nucleic Acids Res 48(D1):D148–D154. https://doi.org/10.1093/nar/gkz896

Ishii D, Kawasaki T, Sato H et al (2024) Effects of anti-fibrotic drugs on transcriptome of peripheral blood mononuclear cells in idiopathic pulmonary fibrosis. Int J Mol Sci 25(7):3750. https://doi.org/10.3390/ijms25073750

Ishtiaq Ahmed AS, Bose GC, Huang L, Azhar M (2014) Generation of mice carrying a knockout-first and conditional-ready allele of transforming growth factor beta2 gene. Genesis 52(9):817–826. https://doi.org/10.1002/dvg.22795

Jiang X, Ning Q (2020) The mechanism of lncRNA H19 in fibrosis and its potential as novel therapeutic target. Mech Ageing Dev 188:111243. https://doi.org/10.1016/j.mad.2020.111243
Jordan NP, Tingle SJ, Shuttleworth VG et al (2021) MiR-126-3p is dynamically regulated in endothelial-to-mesenchymal transition during fibrosis. Int J Mol Sci 22(16):8629. https://doi.org/10.3390/ijms22168629
Kadota T, Fujita Y, Araya J et al (2021) Human bronchial epithelial cell-derived extracellular vesicle therapy for pulmonary fibrosis via inhibition of TGF-β-WNT crosstalk. J Extracell Vesicles 10(10):e12124. https://doi.org/10.1002/jev2.12124
Klicka K, Grzywa TM, Mielniczuk A et al (2022) The role of miR-200 family in the regulation of hallmarks of cancer. Front Oncol 12:965231. https://doi.org/10.3389/fonc.2022.965231
Kolenda T, Guglas K, Kopczyńska M et al (2020) Good or not good: role of miR-18a in cancer biology. Rep Pract Oncol Radiother 25(5):808–819. https://doi.org/10.1016/j.rpor.2020.07.006
Kong Q, Zhou J, Tian G et al (2021) The potential role of long non-coding RNA Dnm3os in the activation of cardiac fibroblasts Sheng Wu Yi Xue Gong Cheng Xue Za Zhi 38(3):574–582. Chinese. https://doi.org/10.7507/1001-5515.202102021
Kopp F, Mendell JT (2018) Functional classification and experimental dissection of long noncoding RNAs. Cell 172(3):393–407. https://doi.org/10.1016/j.cell.2018.01.011
Kp A, Kaliaperumal K, Sekar D (2024) microRNAs and their therapeutic strategy in phase I and phase II clinical trials. Epigenomics 16(4):259–271. https://doi.org/10.2217/epi-2023-0363
Lai X, Zhong J, Zhang A et al (2022) Focus on long non-coding RNA MALAT1: insights into acute and chronic lung diseases. Front Genet 13:1003964. https://doi.org/10.3389/fgene.2022.1003964
Leask A (2013) Focal adhesion kinase: a key mediator of transforming growth factor beta signaling in fibroblasts. Adv Wound Care (New Rochelle) 2(5):247–249. https://doi.org/10.1089/wound.2012.0363
Li X, Yu T, Shan H et al (2018a) lncRNA PFAL promotes lung fibrosis through CTGF by competitively binding miR-18a. FASEB J 32(10):5285–5297. https://doi.org/10.1096/fj.201800055R
Li ZX, Zhu QN, Zhang HB et al (2018b) MALAT1: a potential biomarker in cancer. Cancer Manag Res 10:6757–6768. https://doi.org/10.2147/CMAR.S169406
Li Z, Yi N, Chen R et al (2020) miR-29b-3p protects cardiomyocytes against endotoxin-induced apoptosis and inflammatory response through targeting FOXO3A. Cell Signal 74:109716. https://doi.org/10.1016/j.cellsig.2020.109716
Li H, Tian X, Ruan Y, Xing J, Meng Z (2021) Asiatic acid alleviates Ang-II induced cardiac hypertrophy and fibrosis via miR-126/PIK3R2 signaling. Nutr Metab (Lond) 18(1):71. https://doi.org/10.1186/s12986-021-00596-7
Li H, Li J, Hu Y et al (2023) FOXO3 regulates Smad3 and Smad7 through SPON1 circular RNA to inhibit idiopathic pulmonary fibrosis. Int J Biol Sci 19(10):3042–3056. https://doi.org/10.7150/ijbs.80140
Li JH, Liu S, Zhou H, Qu LH, Yang JH (2014) starBase v2.0: decoding miRNA-ceRNA, miRNA-ncRNA and protein-RNA interaction networks from large-scale CLIP-Seq data. Nucleic Acids Res 42(Database issue):D92-D97. https://doi.org/10.1093/nar/gkt1248
Lin L, Li Q, Hao W et al (2019) Upregulation of LncRNA Malat1 induced proliferation and migration of airway smooth muscle cells via miR-150-eIF4E/Akt Signaling. Front Physiol 10:1337. https://doi.org/10.3389/fphys.2019.01337
Lin X, Zhuang S, Chen X et al (2022) lncRNA ITGB8-AS1 functions as a ceRNA to promote colorectal cancer growth and migration through integrin-mediated focal adhesion signaling. Mol Ther 30(2):688–702. https://doi.org/10.1016/j.ymthe.2021.08.011
Liu Y, Guan H, Zhang JL et al (2018) Acute downregulation of miR-199a attenuates sepsis-induced acute lung injury by targeting SIRT1. Am J Physiol Cell Physiol 314(4):C449–C455. https://doi.org/10.1152/ajpcell.00173.2017
Liu C, Xu Y, Wu X, Zou Q (2019) Clinical significance of Linc00342 expression in the peripheral blood lymphocytes of patients with chronic kidney disease. Int J Nephrol Renovasc Dis 12:251–256. https://doi.org/10.2147/IJNRD.S209832
Liu X, Liu H, Jia X et al (2020) Changing expression profiles of messenger RNA, MicroRNA, long non-coding RNA, and circular RNA (reveal the key regulators and interaction networks of competing endogenous RNA in pulmonary fibrosis. Front Genet 11:558095. https://doi.org/10.3389/fgene.2020.558095

Livak KJ, Schmittgen TD (2001) Analysis of relative gene expression data using real-time quantitative PCR and the 2(-Delta Delta C(T)) method. Methods 25(4):402–408. https://doi.org/10.1006/meth.2001.1262

Long Y, Wang X, Youmans DT, Cech TR (2017) How do lncRNAs regulate transcription? Sci Adv 3(9):eaao2110. https://doi.org/10.1126/sciadv.aao2110

Lu Q, Guo Q, Xin M et al (2021) LncRNA TP53TG1 promotes the growth and migration of hepatocellular carcinoma cells via activation of ERK signaling. Noncoding RNA 7(3):52. https://doi.org/10.3390/ncrna7030052

Mansour SM, El-Abhar HS, Soubh AA (2021) MiR-200a inversely correlates with Hedgehog and TGF-β canonical/non-canonical trajectories to orchestrate the anti-fibrotic effect of Tadalafil in a bleomycin-induced pulmonary fibrosis model. Inflammopharmacology 29(1):167–182. https://doi.org/10.1007/s10787-020-00748-w

McCubbrey AL, Janssen WJ (2024) Using a single-cell atlas of peripheral blood mononuclear cells to understand disease trajectories in idiopathic pulmonary fibrosis. Am J Respir Crit Care Med 210(4):385–387. https://doi.org/10.1164/rccm.202406-1164ED

McGeary SE, Lin KS, Shi CY et al (2019) The biochemical basis of microRNA targeting efficacy. Science 366(6472):eaav1741. https://doi.org/10.1126/science.aav1741

Mehjabin A, Kabir M, Micolucci L et al (2023) MicroRNA in fibrotic disorders: a potential target for future therapeutics. Front Biosci (Landmark Ed) 28(11):317. https://doi.org/10.31083/j.fbl2811317

Miao C, Xiong Y, Zhang G et al (2018) MicroRNAs in idiopathic pulmonary fibrosis, new research progress and their pathophysiological implication. Exp Lung Res 44(3):178–190. https://doi.org/10.1080/01902148.2018.1455927

Michalski JE, Schwartz DA (2021) Genetic risk factors for idiopathic pulmonary fibrosis: insights into immunopathogenesis. J Inflamm Res 13:1305–1318. https://doi.org/10.2147/JIR.S280958

Misharin AV, Morales-Nebreda L, Reyfman PA et al (2017) Monocyte-derived alveolar macrophages drive lung fibrosis and persist in the lung over the life span. J Exp Med 214(8):2387–2404. https://doi.org/10.1084/jem.20162152

Miyoshi K, Yanagi S, Kawahara K et al (2013) Epithelial Pten controls acute lung injury and fibrosis by regulating alveolar epithelial cell integrity. Am J Respir Crit Care Med 187(3):262–275. https://doi.org/10.1164/rccm.201205-0851OC

Moimas S, Salton F, Kosmider B et al (2019) miR-200 family members reduce senescence and restore idiopathic pulmonary fibrosis type II alveolar epithelial cell transdifferentiation. ERJ Open Res 5(4):00138–02019. https://doi.org/10.1183/23120541.00138-2019

Nariman-Saleh-Fam Z, Vahed SZ, Aghaee-Bakhtiari SH et al (2019) Expression pattern of miR-21, miR-25 and PTEN in peripheral blood mononuclear cells of patients with significant or insignificant coronary stenosis. Gene 698:170–178. https://doi.org/10.1016/j.gene.2019.02.074

Noble PW, Barkauskas CE, Jiang D (2012) Pulmonary fibrosis: patterns and perpetrators. J Clin Invest 122(8):2756–2762. https://doi.org/10.1172/JCI60323

Noth I, Zhang Y, Ma SF et al (2013) Genetic variants associated with idiopathic pulmonary fibrosis susceptibility and mortality: a genome-wide association study. Lancet Respir Med 1(4):309–317. https://doi.org/10.1016/S2213-2600(13)70045-6

Pan L, Cheng Y, Yang W et al (2023) Nintedanib ameliorates bleomycin-induced pulmonary fibrosis, inflammation, apoptosis, and oxidative stress by modulating PI3K/Akt/mTOR pathway in mice. Inflammation 46(4):1531–1542. https://doi.org/10.1007/s10753-023-01825-2

Parapuram SK, Thompson K, Tsang M et al (2015) Loss of PTEN expression by mouse fibroblasts results in lung fibrosis through a CCN2-dependent mechanism. Matrix Biol 43:35–41. https://doi.org/10.1016/j.matbio.2015.01.017

Paraskevopoulou MD, Vlachos IS, Karagkouni D et al (2016) DIANA-LncBase v2: indexing microRNA targets on non-coding transcripts. Nucleic Acids Res 44(D1):D231–D238. https://doi.org/10.1093/nar/gkv1270

Pardo A, Selman M (2021) The interplay of the genetic architecture, aging, and environmental factors in the pathogenesis of idiopathic pulmonary fibrosis. Am J Respir Cell Mol Biol 64(2):163–172. https://doi.org/10.1165/rcmb.2020-0373PS

Perez-Favila A, Garza-Veloz I, Hernandez-Marquez LDS et al (2024) Antifibrotic drugs against idiopathic pulmonary fibrosis and pulmonary fibrosis induced by COVID-19: therapeutic approaches and potential diagnostic biomarkers. Int J Mol Sci 25(3):1562. https://doi.org/10.3390/ijms25031562

Phan THG, Paliogiannis P, Nasrallah GK et al (2021) Emerging cellular and molecular determinants of idiopathic pulmonary fibrosis. Cell Mol Life Sci 78(5):2031–2057. https://doi.org/10.1007/s00018-020-03693-7

Podolanczuk AJ, Thomson CC, Remy-Jardin M et al (2013) Idiopathic pulmonary fibrosis: state of the art for 2023. Eur Respir J 61(4):2200957. https://doi.org/10.1183/13993003.00957-2022

Poulet C, Njock MS, Moermans C et al (2020) Exosomal long non-coding RNAs in lung diseases. Int J Mol Sci 21(10):3580. https://doi.org/10.3390/ijms21103580

Qian W, Cai X, Qian Q et al (2019) lncRNA ZEB1-AS1 promotes pulmonary fibrosis through ZEB1-mediated epithelial-mesenchymal transition by competitively binding miR-141-3p. Cell Death Dis 10(2):129. https://doi.org/10.1038/s41419-019-1339-1

Raghu G, Remy-Jardin M, Richeldi L et al (2022) Idiopathic pulmonary fibrosis (an update) and progressive pulmonary fibrosis in adults: an official ATS/ERS/JRS/ALAT clinical practice guideline. Am J Respir Crit Care Med 205(9):e18–e47. https://doi.org/10.1164/rccm.202202-0399ST

Richeldi L, Rubin AS, Avdeev S, Udwadia ZF, Xu ZJ (2015) Idiopathic pulmonary fibrosis in BRIC countries: the cases of Brazil, Russia, India, and China. BMC Med 19(1):220. https://doi.org/10.1186/s12916-021-02111-4

Richeldi L, Collard HR, Jones MG (2017) Idiopathic pulmonary fibrosis. Lancet 389(10082):1941–1952. https://doi.org/10.1016/S0140-6736(17)30866-8

Romero Y, Bueno M, Ramirez R et al (2016) mTORC1 activation decreases autophagy in aging and idiopathic pulmonary fibrosis and contributes to apoptosis resistance in IPF fibroblasts. Aging Cell 15(6):1103–1112. https://doi.org/10.1111/acel.12514

Rosenbloom J, Mendoza FA, Jimenez SA (2013) Strategies for anti-fibrotic therapies. Biochim Biophys Acta 1832(7):1088–1103. https://doi.org/10.1016/j.bbadis.2012.12.007

Savary G, Dewaeles E, Diazzi S et al (2019) The long noncoding RNA DNM3OS is a reservoir of FibromiRs with major functions in lung fibroblast response to TGF-β and pulmonary fibrosis. Am J Respir Crit Care Med 200(2):184–198. https://doi.org/10.1164/rccm.201807-1237OC

Saxton RA, Sabatini DM (2017) mTOR signaling in growth, metabolism, and disease. Cell 168(6):960–976.

Schepers D, Tortora G, Morisaki H et al (2018) A mutation update on the LDS-associated genes TGFB2/3 and SMAD2/3. Hum Mutat 39(5):621–634. https://doi.org/10.1002/humu.23407

Schott CA, Ascoli C, Huang Y et al (2020) Declining pulmonary function in interstitial lung disease linked to lymphocyte dysfunction. Am J Respir Crit Care Med 201(5):610–613. https://doi.org/10.1164/rccm.201910-1909LE

Schumacher S, Vazquez Nunez R, Biertümpfel C et al (2022) Bottom-up reconstitution of focal adhesion complexes. FEBS J 289(12):3360–3373. https://doi.org/10.1111/febs.16023

Scott MKD, Quinn K, Li Q et al (2019) Increased monocyte count as a cellular biomarker for poor outcomes in fibrotic diseases: a retrospective, multicentre cohort study. Lancet Respir Med 7(6):497–508. https://doi.org/10.1016/S2213-2600(18)30508-3

Seyhan AA (2024) Trials and tribulations of MicroRNA therapeutics. Int J Mol Sci 25(3):1469. https://doi.org/10.3390/ijms25031469

Shan Y, Chen Y, Brkić J et al (2022) miR-218-5p induces interleukin-1β and endovascular trophoblast differentiation by targeting the transforming growth factor β-SMAD2 pathway. Front Endocrinol (Lausanne) 13:842587. https://doi.org/10.3389/fendo.2022.842587

Shao M, Ma H, Wan X, Liu Y (2020) Survival analysis for long noncoding RNAs identifies TP53TG1 as an antioncogenic target for the breast cancer. J Cell Physiol 235(10):6574–6581. https://doi.org/10.1002/jcp.29517

Shen K, Cao Z, Zhu R, You L, Zhang T (2019) The dual functional role of MicroRNA-18a (miR-18a) in cancer development. Clin Transl Med 8(1):32. https://doi.org/10.1186/s40169-019-0250-9

Shen Y, Zhu Y, Rong F (2020) miR-200c-3p regulates the proliferation and apoptosis of human trabecular meshwork cells by targeting PTEN. Mol Med Rep 22(2):1605–1612. https://doi.org/10.3892/mmr.2020.11198

Smyth A, Callaghan B, Willoughby CE, O'Brien C (2022) The role of miR-29 family in TGF-β driven fibrosis in glaucomatous optic neuropathy. Int J Mol Sci 23(18):10216. https://doi.org/10.3390/ijms231810216

Sodagar H, Alipour S, Hassani S et al (2022) The role of microRNAs in COVID-19 with a focus on miR-200c. J Circ Biomark 11:14–23. https://doi.org/10.33393/jcb.2022.2356

Song B, Ye L, Wu S, Jing Z (2020) Long non-coding RNA MEG3 regulates CSE-induced apoptosis and inflammation via regulating miR-218 in 16HBE cells. Biochem Biophys Res Commun 521(2):368–374. https://doi.org/10.1016/j.bbrc.2019.10.135

Spagnolo P, Lee JS (2023) Recent advances in the genetics of idiopathic pulmonary fibrosis. Curr Opin Pulm Med 29(5):399–405. https://doi.org/10.1097/MCP.0000000000000989

Stefanetti RJ, Voisin S, Russell A, Lamon S (2018) Recent advances in understanding the role of FOXO3. F1000Res 7:F1000 Faculty Rev-1372. https://doi.org/10.12688/f1000research.15258.1

Su H, Yu S, Sun F et al (2022) LINC00342 induces metastasis of lung adenocarcinoma by targeting miR-15b/TPBG. Acta Biochim Pol 69(2):291–297. https://doi.org/10.18388/abp.2020_5697

Sun J, Guo Y, Chen T et al (2022) Systematic analyses identify the anti-fibrotic role of lncRNA TP53TG1 in IPF. Cell Death Dis 13(6):525. https://doi.org/10.1038/s41419-022-04975-7

Tang H, Zhao L, Li M et al (2019) Investigation of LINC00342 as a poor prognostic biomarker for human patients with non-small cell lung cancer. J Cell Biochem 120(4):5055–5061. https://doi.org/10.1002/jcb.27782

Tanni SE, Fabro AT, de Albuquerque A et al (2021) Pulmonary fibrosis secondary to COVID-19: a narrative review. Expert Rev Respir Med 15(6):791–803. https://doi.org/10.1080/17476348.2021.1916472

Tao J, Wang J, Li C et al (2019) MiR-216a accelerates proliferation and fibrogenesis via targeting PTEN and SMAD7 in human cardiac fibroblasts. Cardiovasc Diagn Ther 9(6):535–544. https://doi.org/10.21037/cdt.2019.11.06

Tepebaşı MY, Öztürk MY (2023) miR-21, miR-221, and miR-222 upregulation in lung cancer promotes metastasis by reducing oxidative stress and apoptosis. Rev Assoc Med Bras 69(6):e20221688. https://doi.org/10.1590/1806-9282.20221688

Tian Y, Li H, Qiu T et al (2019) Loss of PTEN induces lung fibrosis via alveolar epithelial cell senescence depending on NF-κB activation. Aging Cell 18(1):e12858. https://doi.org/10.1111/acel.12858

Tirelli C, Pesenti C, Miozzo M et al (2022) The genetic and epigenetic footprint in idiopathic pulmonary fibrosis and familial pulmonary fibrosis: a state-of-the-art review. Diagnostics (Basel) 12(12):3107. https://doi.org/10.3390/diagnostics12123107

Unterman A, Zhao AY, Neumark N et al (2024) Single-cell profiling reveals immune aberrations in progressive idiopathic pulmonary fibrosis. Am J Respir Crit Care Med 210(4):484–496. https://doi.org/10.1164/rccm.202306-0979OC

Usman K, Hsieh A, Hackett TL (2021) The role of miRNAs in extracellular matrix repair and chronic fibrotic lung diseases. Cells 10(7):1706. https://doi.org/10.3390/cells10071706

Usman Pp AS, Sekar D (2024) microRNA-based electrochemical biosensor for early detection of pulmonary arterial hypertension. Hypertens Res 47(7):2000–2002. https://doi.org/10.1038/s41440-024-01719-2

Wang L, Chen Z, An L et al (2016) Analysis of long non-coding RNA expression profiles in non-small cell lung cancer. Cell Physiol Biochem 38(6):2389–2400. https://doi.org/10.1159/000445591

Wang R, Zhang M, Ou Z et al (2019a) Long noncoding RNA DNM3OS promotes prostate stromal cells transformation via the miR-29a/29b/COL3A1 and miR-361/TGFβ1 axes. Aging (Albany) 11(21):9442–9460. https://doi.org/10.18632/aging.102395

Wang S, Ni B, Zhang Z et al (2019b) Long non-coding RNA DNM3OS promotes tumor progression and EMT in gastric cancer by associating with Snail. Biochem Biophys Res Commun 511(1):57–62. https://doi.org/10.1016/j.bbrc.2019.02.030

Wang F, Li P, Li FS (2020) Integrated analysis of a gene correlation network identifies critical regulation of fibrosis by lncRNAs and TFs in idiopathic pulmonary fibrosis. Biomed Res Int 2020:6537462. https://doi.org/10.1155/2020/6537462

Wang Y, Mou Q, Zhu Z, Zhao L, Zhu L (2021) MALAT1 promotes liver fibrosis by sponging miR-181a and activating TLR4-NF-κB signaling. Int J Mol Med 48(6):215. https://doi.org/10.3892/ijmm.2021.5048

Wang J, Hu K, Cai X et al (2022) Targeting PI3K/AKT signaling for treatment of idiopathic pulmonary fibrosis. Acta Pharm Sin B 12(1):18–32. https://doi.org/10.1016/j.apsb.2021.07.023

Wang S, Sun Y, Yao L et al (2024) The role of microRNA-23a-3p in the progression of human aging process by targeting FOXO3a. Mol Biotechnol 66(2):277–287. https://doi.org/10.1007/s12033-023-00746-7

Wheaton AK, Agarwal M, Jia S et al (2017) Lung epithelial cell focal adhesion kinase signaling inhibits lung injury and fibrosis. Am J Physiol Lung Cell Mol Physiol 312(5):L722–L730. https://doi.org/10.1152/ajplung.00478.2016

Wu M, Huang Y, Chen T et al (2019) LncRNA MEG3 inhibits the progression of prostate cancer by modulating miR-9-5p/QKI-5 axis. J Cell Mol Med 23(1):29–38. https://doi.org/10.1111/jcmm.13658

Wynn TA, Vannella KM (2016) Macrophages in tissue repair, regeneration, and fibrosis. Immunity 44(3):450–462. https://doi.org/10.1016/j.immuni.2016.02.015

Xia H, Khalil W, Kahm J et al (2010) Pathologic caveolin-1 regulation of PTEN in idiopathic pulmonary fibrosis. Am J Pathol 176(6):2626–2637. https://doi.org/10.2353/ajpath.2010.091117

Xiao XH, He SY (2020) ELF1 activated long non-coding RNA CASC2 inhibits cisplatin resistance of non-small cell lung cancer via the miR-18a/IRF-2 signaling pathway. Eur Rev Med Pharmacol Sci 24(6):3130–3142. https://doi.org/10.26355/eurrev_202003_20680

Xiao H, Liu Y, Liang P et al (2018) TP53TG1 enhances cisplatin sensitivity of non-small cell lung cancer cells through regulating miR-18a/PTEN axis. Cell Biosci 8:23. https://doi.org/10.1186/s13578-018-0221-7

Xu Q, Cheng D, Liu Y et al (2021) LncRNA-ATB regulates epithelial-mesenchymal transition progression in pulmonary fibrosis via sponging miR-29b-2-5p and miR-34c-3p. J Cell Mol Med 25(15):7294–7306. https://doi.org/10.1111/jcmm.16758

Xu Y, Lan P, Wang T (2023) The role of immune cells in the pathogenesis of idiopathic pulmonary fibrosis. Medicina (Kaunas) 59(11):1984. https://doi.org/10.3390/medicina59111984

Xue R, Li Y, Li X et al (2019) miR-185 affected the EMT, cell viability, and proliferation via DNMT1/MEG3 pathway in TGF-β1-induced renal fibrosis. Cell Biol Int 43(10):1152–1162. https://doi.org/10.1002/cbin.11046

Yan W, Wu Q, Yao W et al (2017) MiR-503 modulates epithelial-mesenchymal transition in silica-induced pulmonary fibrosis by targeting PI3K p85 and is sponged by lncRNA MALAT1. Sci Rep 7(1):11313. https://doi.org/10.1038/s41598-017-11904-8

Yang IV, Luna LG, Cotter J et al (2012a) The peripheral blood transcriptome identifies the presence and extent of disease in idiopathic pulmonary fibrosis. PLoS ONE 7(6):e37708. https://doi.org/10.1371/journal.pone.0037708

Yang S, Banerjee S, de Freitas A et al (2012b) Participation of miR-200 in pulmonary fibrosis. Am J Pathol 180(2):484–493. https://doi.org/10.1016/j.ajpath.2011.10.005

Yang J, Qi M, Fei X et al (2021a) LncRNA H19: a novel oncogene in multiple cancers. Int J Biol Sci 17(12):3188–3208. https://doi.org/10.7150/ijbs.62573

Yang YL, Chang YH, Li CJ et al (2021b) New insights into the role of miR-29a in hepatocellular carcinoma: implications in mechanisms and theragnostics. J Pers Med 11(3):219. https://doi.org/10.3390/jpm11030219(b)

Ye Z, Hu Y (2021) TGF-β1: gentlemanly orchestrator in idiopathic pulmonary fibrosis (review). Int J Mol Med 48(1):132. https://doi.org/10.3892/ijmm.2021.4965

Yin X, Yin Y, Dai L et al (2021) Integrated analysis of long non-coding RNAs and mRNAs associated with malignant transformation of gastrointestinal stromal tumors. Cell Death Dis 12(7):669. https://doi.org/10.1038/s41419-021-03942-y

Yu J, Chen J, Yang H et al (2019) Overexpression of miR-200a-3p promoted inflammation in sepsis-induced brain injury through ROS-induced NLRP3. Int J Mol Med 44(5):1811–1823. https://doi.org/10.3892/ijmm.2019.4326

Yu WK, Chen WC, Su VY et al (2022) Nintedanib inhibits endothelial mesenchymal transition in bleomycin-induced pulmonary fibrosis via focal adhesion kinase activity reduction. Int J Mol Sci 23(15):8193. https://doi.org/10.3390/ijms23158193

Yu F, Geng W, Dong P et al (2018) LncRNA-MEG3 inhibits activation of hepatic stellate cells through SMO protein and miR-212 [published correction appears in Cell Death Dis. 2022 Feb 9;13(2):133. https://doi.org/10.1038/s41419-022-04558-6]. Cell Death Dis 9(10):1014. https://doi.org/10.1038/s41419-018-1068-x

Yu H, Qi N, Zhou Q (2021) LncRNA H19 inhibits proliferation and migration of airway smooth muscle cells induced by PDGF-BB through miR-21/PTEN/Akt axis. J Asthma Allergy 14:71–80. https://doi.org/10.2147/JAA.S291333

Yuan J, Jiang YY, Mayakonda A et al (2017) Super-enhancers promote transcriptional dysregulation in nasopharyngeal carcinoma. Cancer Res 77(23):6614–6626. https://doi.org/10.1158/0008-5472.CAN-17-1143

Yue B, Xiong D, Chen J et al (2024) SPP1 induces idiopathic pulmonary fibrosis and NSCLC progression via the PI3K/Akt/mTOR pathway. Respir Res 25(1):362. https://doi.org/10.1186/s12931-024-02989-7

Zhan H, Sun X, Wang X et al (2021) LncRNA MEG3 involved in NiO NPs-induced pulmonary fibrosis via regulating TGF-β1-mediated PI3K/AKT pathway. Toxicol Sci 182(1):120–131. https://doi.org/10.1093/toxsci/kfab047

Zhang Q, Ye H, Xiang F et al (2017a) miR-18a-5p inhibits sub-pleural pulmonary fibrosis by targeting TGF-β receptor II. Mol Ther 25(3):728–738. https://doi.org/10.1016/j.ymthe.2016.12.017

Zhang X, Hamblin MH, Yin KJ (2017b) The long noncoding RNA Malat 1: its physiological and pathophysiological functions. RNA Biol 14(12):1705–1714. https://doi.org/10.1080/15476286.2017.1358347

Zhang P, Wu W, Chen Q, Chen M (2019) Non-coding RNAs and their integrated networks. J Integr Bioinform 16(3):20190027. https://doi.org/10.1515/jib-2019-0027

Zhang S, Chen H, Yue D et al (2021) Long non-coding RNAs: promising new targets in pulmonary fibrosis. J Gene Med 23(3):e3318. https://doi.org/10.1002/jgm.3318

Zhao Y, Li A (2021) miR-19b-3p relieves intervertebral disc degeneration through modulating PTEN/PI3K/Akt/mTOR signaling pathway. Aging (Albany) 13(18):22459–22473. https://doi.org/10.18632/aging.203553

Zhong B, Yin Z, Guo X et al (2023) High expression of FOXO3 in gastric cancer tissues is associated with poor prognosis and immune cell infiltration. Clin Lab. https://doi.org/10.7754/Clin.Lab.2023.230219

Zhou L, Li P, Zhang M et al (2020) Carbon black nanoparticles induce pulmonary fibrosis through NLRP3 inflammasome pathway modulated by miR-96 targeted FOXO3a. Chemosphere 241:125075. https://doi.org/10.1016/j.chemosphere.2019.125075

Zhu J, Chen G, Zhu S et al (2016) Identification of tissue-specific protein-coding and noncoding transcripts across 14 human tissues using RNA-seq. Sci Rep 6:28400. https://doi.org/10.1038/srep28400

Authors and Affiliations

Gulnaz F. Korytina[1,2] · Vitaly A. Markelov[1,2] · Irshat A. Gibadullin[2] · Shamil R. Zulkarneev[2] · Timur R. Nasibullin[1] · Rustem H. Zulkarneev[2] · Arthur M. Avzaletdinov[2] · Sergey N. Avdeev[3] · Naufal Sh. Zagidullin[2]

✉ Gulnaz F. Korytina
guly_kory@mail.ru

[1] Institute of Biochemistry and Genetics—Subdivision of the Ufa Federal Research Centre of the Russian Academy of Sciences (IBG UFRC RAS), Pr. Oktyabrya, 71, Ufa 450054, Russian Federation

[2] Bashkir State Medical University, Lenina Str. 3, Ufa 450008, Russian Federation

[3] Sechenov First Moscow State Medical University (Sechenov University), 8-2, Trubetskaya Str., Moscow 119991, Russian Federation